ric HCVs based on the JFH1 strain (21) and an infectious clone of genotype 1a, H77S, that produces fewer infectious particles than the genotype 2a JFH1 strain (68), propagation of HCV was still limited to Huh7 cells. Exogenous expression of miR122 has been shown to support HCV RNA replication in a human embryonic kidney epithelial cell line and mouse embryonic fibroblasts (7, 35), and we therefore thought that the possibility of complete propagation of HCVcc in various human liver cell lines by the expression of miR122 needed to be examined. Among the cell lines that we examined, Hep3B cells, which were established from human liver tumor biopsy samples in 1976 (1) and have been well characterized as model liver cells in various fields of research (47, 55, 63, 67), were shown to support the efficient propagation of HCVcc comparable to that in Huh7 cells by the expression of miR122. Establishment of novel cell culture systems through the exogenous expression of miR122 provides a clue to understanding the precise roles of miR122 in the life cycle of HCV.

MATERIALS AND METHODS

Plasmids. The cDNA clones of wild-type miR122 (WT-miR122), single mutant miR122 (sMT-miR122), double mutant miR122 (dMT-miR122), *Aequorea coerulescens* green fluorescent protein (AcGFP), and claudin-1 (CLDN) were inserted between the XhoI and XbaI sites of a lentiviral vector, pCSII-EF-RfA, which was kindly provided by M. Hijikata, and the resulting plasmids were designated pCSII-EF-WT-miR122, pCSII-EF-sMT-miR122, pCSII-EF-dMT-miR122, pCSII-EF-AcGFP, and pCSII-EF-Claudin1, respectively. pHH-JFH1 was kindly provided by T. Wakita (39). pHH-JFH1-E2p7NS2mt contains three adaptive mutations in pHH-JFH1 (53). pFGR-JFH1 and pSGR-JFH1 encoded a full-length and a subgenomic cDNA of the JFH1 strain, respectively. The complementary sequence of miR122 was inserted into the PmeI site of the pmirGLO vector (Promega, Madison, WI), and the resulting plasmid was designated pmirGLO-miR122comp. pIFNβ-Luc and pISRE-Luc carrying a firefly luciferase gene under the control of the beta IFN (IFN-β) and interferon-sensitive response element (ISRE) promoters, respectively, were kindly provided by T. Kawai and S. Akira. The internal control plasmid encoding a *Renilla* luciferase (pRL-TK) was purchased from Promega. The plasmids used in this study were confirmed by sequencing with an ABI Prism 3130 genetic analyzer (Applied Biosystems, Tokyo, Japan).

Cells. All cell lines were cultured at 37°C under the condition of a humidified atmosphere and 5% CO_2. The human embryonic kidney 293T cell line and hepatocellular carcinoma cell lines Huh7, Huh6/CLDN, HepG2/CD81, Hep3B, and PKC/PRL/5 were maintained in Dulbecco's modified Eagle's medium (DMEM; Sigma, St. Louis, MO) supplemented with 100 U/ml penicillin, 100 μg/ml streptomycin, and 10% fetal calf serum (FCS). HepG2/CD81 cells were generated as described previously (60). Huh6 cells were transduced with a lentiviral vector expressing claudin-1, and the resulting cells were designated Huh6/CLDN. The Huh7-derived cell line Huh7.5.1 was kindly provided by F. Chisari and was maintained in DMEM containing nonessential amino acids (NEAA), 100 U/ml penicillin, 100 μg/ml streptomycin, and 10% FCS. Hep3B replicon cells harboring the subgenomic HCV RNA were maintained in DMEM containing 10% FCS, NEAA, and 400 μg/ml G418 (Nakalai Tesque, Kyoto, Japan).

Viruses. pHH-JFH1-E2p7NS2mt was transfected into Huh7.5.1 cells, and the culture supernatants were collected after serial passages. The infectivity of HCVcc was determined by focus-forming assay and expressed in focus-forming units (FFU) (64). The lentiviral vectors and ViraPower lentiviral packaging mix (Invitrogen, San Diego, CA) were cotransfected into 293T cells, and the supernatants were recovered at 48 h posttransfection. The culture supernatants were centrifuged at 1,000 × g for 5 min and cleared through a 0.45-μm-pore-size filter. The lentivirus titer was determined by a Lenti-X quantitative reverse transcription (qRT)-PCR titration kit (Clontech, Mountain View, CA). The vesicular stomatitis virus

(VSV) variant NCP12.1, derived from the Indiana strain, was kindly provided by M. Whitt. Pseudotype VSVs bearing the HCV E1 and E2 glycoproteins (HCVpv) and VSV G protein (VSVpv) were prepared as described previously (60). The infectivity of the pseudotype viruses was assessed by the expression of luciferase, determined by a Bright-Glo luciferase assay system (Promega) following a protocol provided by the manufacturer and expressed in relative light units (RLU).

Reagents and antibodies. Cyclosporine (CsA) and human recombinant IFN-α2 were purchased from Sigma and R&D Systems (Minneapolis, MN), respectively. BODIPY 558/568 lipid probe was purchased from Invitrogen. Poly(I·C) was purchased from InvivoGen (San Diego, CA). LNAs complementary to miR122 (LNA-miR122; 5'-CcAttGTcaCaCtCC-3') and its negative control (LNA-Cont; 5'-CcAttCTgaCcCtAC-3') (LNA in capital letters, DNA in lowercase letters; sulfur atoms in oligonucleotide phosphorothioates are substituted for nonbridging oxygen atoms; capital C indicates LNA methylcytosine) (14) were purchased from Gene Design (Osaka, Japan). miScript miRNA mimics hsa-miR122 and its negative control were purchased from Qiagen (Valencia, CA). Mouse monoclonal antibodies to HCV NS5A and β-actin were purchased from Austral Biologicals (San Ramon, CA) and Sigma, respectively. Mouse anti-apolipoprotein E (anti-ApoE), rabbit anti-diacylglycerol acyltransferase 1 (DGAT1), rabbit anti-signal transducer and activators of transcription 2 (anti-STAT2), and rabbit anti-IFN regulatory factor 3 (anti-IRF3) antibodies were purchased from Santa Cruz (Santa Cruz, CA). Rabbit anti-HCV core protein was prepared as described previously (45). Phycoerythrin (PE)-conjugated anti-human CD81 (anti-hCD81) and anti-mouse IgG antibodies were purchased from BD Biosciences (Franklin Lakes, NJ). Mouse anti-double-stranded RNA (anti-dsRNA) IgG2a (J1 and K2) antibodies were from Biocenter Ltd. (Szirak, Hungary). Alexa Fluor 488 (AF488)-conjugated anti-mouse and -rabbit IgG and AF594-conjugated anti-rabbit IgG antibodies were from Invitrogen.

Quantitative RT-PCR. For quantitation of HCV RNA, total RNA was prepared from cells by using an RNeasy minikit (Qiagen). The synthesis of a first-stranded cDNA and quantitative RT-PCR were performed using TaqMan EZ RT-PCR core reagents and an ABI Prism 7000 system (Applied Biosystems) according to the manufacturer's protocol. For quantitation of miRNA, total RNA was prepared from cells by using an miRNeasy minikit (Qiagen), and miR122 was estimated by using miR122-specific RT primers and amplified using specific primers provided in the TaqMan MicroRNA assays (Applied Biosystems) according to the manufacturer's protocol. U6 small nuclear RNA (snRNA) was used as an internal control. Fluorescent signals were analyzed by an ABI Prism 7000 system (Applied Biosystems).

Transfection and immunoblotting. Cells were transfected with the plasmids by using *Trans* IT LT-1 (Mirus, Madison, WI) or Lipofectamine 2000 (Invitrogen) according to the manufacturers' protocols. Cells were lysed on ice in Triton lysis buffer (20 mM Tris-HCl [pH 7.4], 135 mM NaCl, 1% Triton X-100, 10% glycerol) supplemented with a protease inhibitor mix (Nacalai Tesque). The samples were boiled in loading buffer and subjected to 5 to 20% gradient sodium dodecyl sulfate-polyacrylamide gel electrophoresis (SDS-PAGE). The proteins were transferred to polyvinylidene difluoride membranes (Millipore, Bedford, MA) and reacted with primary antibody and then secondary horseradish peroxidase-conjugated antibody. The immunocomplexes were visualized with Super Signal West Femto substrate (Pierce, Rockford, IL) and detected by using an LAS-3000 image analyzer (Fujifilm, Tokyo, Japan).

Indirect immunofluorescence assay. Cells cultured on glass slides were fixed with 4% paraformaldehyde in phosphate-buffered saline (PBS) at room temperature for 30 min. After washing three times with PBS, the cells were permeabilized for 20 min at room temperature with PBS containing 0.25% saponin and blocked with phosphate buffer containing 2% bovine serum albumin (BSA) for 1 h at room temperature. The cells were incubated with blocking buffer containing mouse anti-dsRNA, rabbit anti-NS5A, rabbit anti-core, rabbit anti-IRF3, or rabbit anti-STAT2 at room temperature for 1 h, washed three times with PBS, and incubated

40
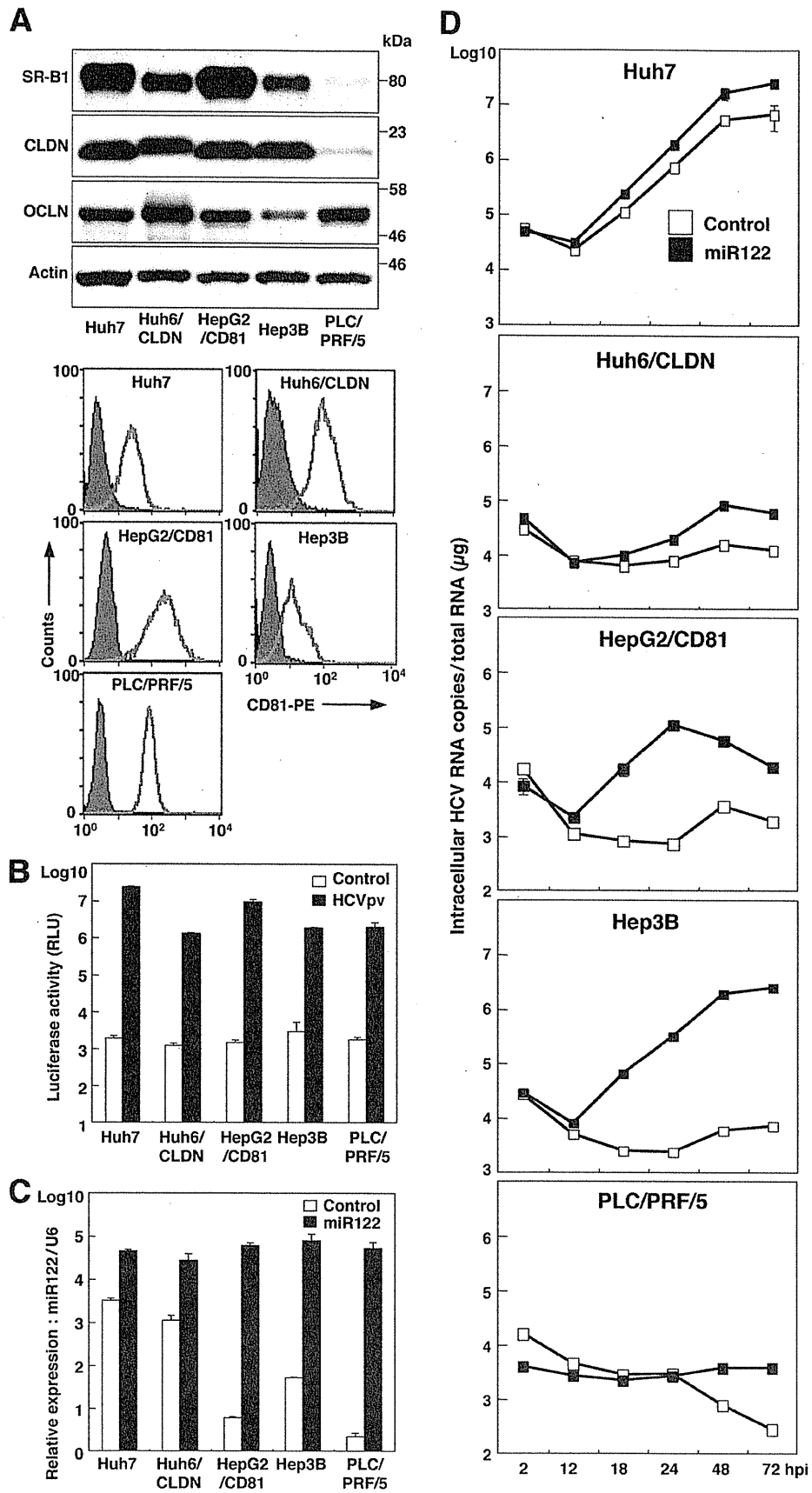
with blocking buffer containing appropriate AF488-conjugated and AF594-conjugated secondary antibodies at room temperature for 1 h. Finally, the cells were washed three times with PBS and observed with a FluoView FV1000 laser scanning confocal microscope (Olympus, Tokyo, Japan).

Flow cytometry. Cultured cells were detached with 0.25% trypsin-EDTA and incubated with PE-conjugated anti-hCD81 antibody or anti-mouse IgG antibody for 1 h at 4°C. After being washed twice with PBS containing 1% BSA, the cells were analyzed by a BD FACSCalibur flow cytometry system (BD Biosciences).

In vitro **transcription, RNA transfection, and colony formation.** The plasmids pSGR-JFH1 and pFGR-JFH1 were linearized with XbaI and treated with mung bean exonuclease. The linearized DNA was transcribed *in vitro* by using a MEGAscript T7 kit (Applied Biosystems) according to the manufacturer's protocol. The *in vitro*-transcribed RNA (10 μg) was electroporated into Hep3B cells at 10^6 cells/0.4 ml under conditions of 270 V and 960 μF using a Gene Pulser apparatus (Bio-Rad, Hercules, CA) and plated on DMEM containing 10% FCS and NEAA. The medium was replaced with fresh DMEM containing 10% FCS, NEAA, and 400 μg/ml G418 at 24 h posttransfection. The remaining colonies were fixed with 4% paraformaldehyde and stained with crystal violet at 1 month postelectroporation.

Luciferase assay. Cells were seeded onto 24-well plates at a concentration of 5×10^4 cells/well and transfected with 250 ng of each of the plasmids. At 24 h posttransfection, cells were stimulated with the appropriate ligands for 24 h and then lysed in 100 μl of passive lysis buffer (Promega). Luciferase activity was measured in 20-μl aliquots of the cell lysates using a dual-luciferase reporter assay system (Promega). Firefly luciferase activity was standardized with that of *Renilla* luciferase cotransfected with the internal control plasmid pRL-TK and was expressed as RLU.

RESULTS

Expression of miR122 facilitates replication of HCVcc in various liver cell lines. The robust *in vitro* cell culture systems for HCV use the HCV genotype 2a isolate JFH1 and Huh7-derived cell lines (64). To expand the host range of HCVcc to gain more insight into the host-virus interaction, we examined the effect of expression of miR122, a liver-specific microRNA that was shown to be crucial for the efficient replication of HCV (27–29, 38, 52), in several well-characterized liver cell lines: Huh6, HepG2, Hep3B, and PLC/PRF/5. Although hCD81, SR-B1, claudin-1 (CLDN), and occludin (OCLN) are known to be crucial for entry of HCVcc (15, 48, 49, 54), the Huh6 and HepG2 cell lines express little or no CLDN and hCD81 (10, 22), respectively. Therefore, CLDN and hCD81 were exogenously expressed in the cell lines, and the resulting lines were designated Huh6/CLDN and HepG2/CD81, respectively. Expression of the receptor molecules in the cell lines was confirmed by immunoblot and fluorescence-activated cell sorter (FACS) analyses (Fig. 1A). To further examine the susceptibility to HCV infection, pseudotyped VSV bearing the HCV envelope protein, HCVpv, was inoculated into these cell lines. Significant expression of luciferase was observed in these cell lines upon infection with HCVpv but not upon infection with the con-

trol virus (Fig. 1B), suggesting that the liver cell lines express functional receptors required for entry of HCV. To determine the effect of miR122 on the replication of HCVcc, we next assessed the level of miR122 in the liver cell lines by qRT-PCR. Although miR122 is highly expressed in the liver (13), the expression level of miR122 varied among the liver cell lines (Fig. 1C, white bars). To examine the effect of the exogenous expression of miR122 in the liver cell lines on the replication of HCVcc, miR122 was expressed in the cell lines by the lentiviral vector. The expression level of miR122 in the liver cell lines, including Huh7 cells, was shown to be upregulated to a significantly greater extent than that in Huh7 cells alone (Fig. 1C, black bars). To examine the effect of miR122 on the replication of HCV, HCVcc was inoculated into the cell lines (Fig. 1D). Although Huh7 cells exhibited an efficient HCV replication, a slight enhancement of the replication was observed by the expression of miR122. No HCV replication was observed in PLC/PRF/5 cells irrespective of miR122 expression. Hep3B and HepG2/CD81 cells exhibited a significant enhancement of HCV replication by the expression of miR122, in contrast to a slight increase in Huh6/CLDN cells. Notably, HCV RNA levels were drastically increased by more than 300-fold at 72 h postinfection in Hep3B cells by the expression of miR122, suggesting that Hep3B is the most suitable cell line for investigating the biological significance of miR122 on the propagation of HCV and for establishing a permissive cell line for HCVcc. Therefore, we used Hep3B cells overexpressing miR122 (Hep3B/miR122 cells) for further experiments.

Expression of biologically active miR122 facilitates replication of HCVcc in Hep3B cells. To confirm the activity of endogenously and exogenously expressed miR122 to suppress the translation in cells, a pmirGLO vector carrying the complementary sequence of miR122 under the luciferase gene was transfected into Huh7 cells, Hep3B cells expressing AcGFP (Hep3B/Cont), and Hep3B/miR122 cells. Suppression of luciferase expression was observed in Huh7 and Hep3B/miR122 cells but not in Hep3B/Cont cells (Fig. 2A), suggesting that miR122 exogenously expressed in Hep3B cells is as biologically active as that endogenously expressed in Huh7 cells. To determine the effect of miR122 on the propagation of HCVcc, Hep3B cells were infected with the lentiviral vector expressing miR122 and then inoculated with HCVcc. The levels of HCV RNA in Hep3B cells upon infection with HCVcc were increased in proportion to the amount of lentiviral vector (Fig. 2B). Recently, an inhibitor for miR122, SPC3649, which is an LNA in which 2' oxygen and 4' carbon are connected via methylene units, has been shown to possess potent anti-HCV activity in chimpanzees chronically infected with HCV (31). We next examined the effect of LNA on the replication of HCVcc in Huh7 and Hep3B/miR122 cells. HCV RNA replication in Huh7 and Hep3B/miR122 cells was significantly and dose-dependently decreased by treatment with LNA-miR122 but not treatment with LNA-Cont (Fig. 2C). We further investigated the effect of the

FIG 1 Expression of miR122 facilitates replication of HCVcc in various liver cell lines. (A) Human liver cell lines Huh7, Huh6/CLDN, HepG2/CD81, Hep3B, and PLC/PRF/5 were lysed and subjected to immunoblotting using appropriate antibodies. The expression levels of hCD81 in the liver cell lines were determined by flow cytometry. (B) The human liver cell lines were inoculated with HCVpv or control virus and washed three times after 2 h of incubation. Luciferase activities were determined at 24 h postinfection. (C) The cell lines were transduced with lentiviral vectors expressing miR122 or AcGFP as a control. After serial passages, total RNA was extracted from the cells and relative expression of miR122 was determined by qRT-PCR by using U6 snRNA as an internal control. (D) The cells expressing miR122 or control were infected with HCVcc at an MOI of 1. Total RNA was extracted from the cells at the indicated time and subjected to qRT-PCR analysis. The data are representative of three independent experiments. Error bars indicate the standard deviation of the mean.
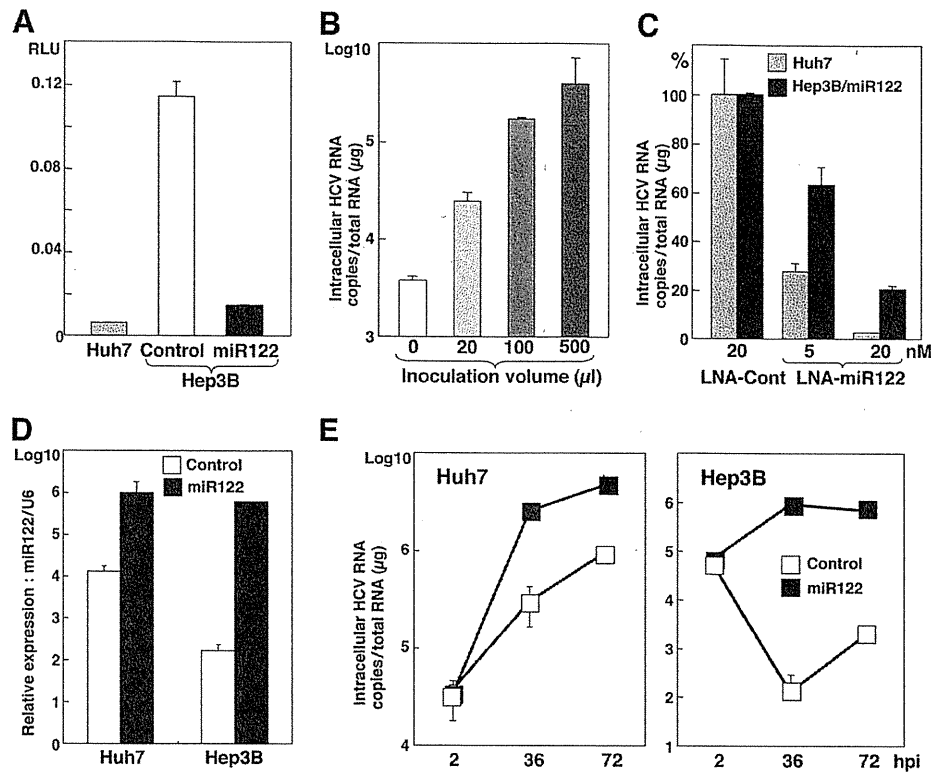
4 1

FIG 2 Expression of biologically active miR122 facilitates replication of HCVcc in Hep3B cells. (A) Huh7, Hep3B/Cont, and Hep3B/miR122 cells were transfected with pmirGLO-miR122comp, and luciferase activity was determined at 24 h posttransfection. (B) Hep3B cells were transduced with the lentiviral vector expressing miR122 in a dose-dependent manner and then infected with HCVcc at an MOI of 1 at 48 h postransduction. Total RNA was extracted from the cells at 72 h postinfection and subjected to qRT-PCR. (C) LNA-Cont (20 nM) or LNA-miR122 (5 nM or 20 nM) was introduced into Hep3B/miR122 cells and infected with HCVcc at an MOI of 1 at 12 h posttransfection. Total RNA was extracted from the cells at 24 h postinfection and subjected to qRT-PCR. (D) Huh7 and Hep3B cells were transfected with mimic miR122 (20 nM) or a negative control (20 nM), and total miRNA was determined by qRT-PCR at 24 h posttransfection. (E) Huh7 and Hep3B cells were transfected with mimic miR122 (20 nM) or a negative control (20 nM) and infected with HCVcc at an MOI of 1 at 12 h posttransfection. Total RNA was extracted from the cells at the indicated time (hpi, hours postinfection) and subjected to qRT-PCR.

mimic miR122, the synthetic double-stranded RNA oligonucleotides that mimic endogenous miRNA function, on the propagation of HCV. Huh7 and Hep3B cells transfected with mimic miR122 but not those transfected with the negative control exhibited a high level of expression of miR122 (Fig. 2D) and enhanced RNA replication upon infection with HCVcc (Fig. 2E). Collectively, these results clearly indicate that expression of biologically active miR122 plays a crucial role in the replication of HCV in Hep3B cells.

Establishment of a novel permissive cell line for robust propagation of HCVcc by expression of miR122 in Hep3B cells. We next examined the possibility of establishing a permissive cell line for the robust propagation of HCVcc by the expression of miR122 in Hep3B cells. Huh7, Hep3B/miR122, and Hep3B/Cont cells were infected with HCVcc, and the levels of expression of HCV NS5A and core proteins were assessed by immunoblotting at 72 h postinfection. Expression of the viral proteins in Hep3B/miR122 cells was almost comparable to that in Huh7 cells, in contrast to no expression in Hep3B/Cont cells (Fig. 3A). Small foci stained by immunofluorescence assay appeared at 24 h postinfection in Hep3B/miR122 and Huh7 cells but not in Hep3B/Cont cells and grew into large foci at 72 h postinfection, indicating that infectious particles are generated in Hep3B/miR122 cells and the progeny particles expand infection to the neighboring cells (Fig. 3B). The

morphology of Hep3B cells is completely different from that of Huh7 cells, and thus, these results are not due to contamination of Huh7 cells. DGAT1 and ApoE have been shown to play crucial roles in the recruitment of core protein to the lipid droplets and viral infectivity, respectively (9, 24). Higher levels of expression of ApoE and DGAT1 were detected in Hep3B cells than in Huh7 cells (Fig. 3C). Furthermore, the concentration of infectious particles recovered in the culture supernatant of Hep3B/miR122 cells infected with HCVcc at a multiplicity of infection (MOI) of 1 at 72 h postinfection was approximately 5 × 10⁴ FFU/ml, which was comparable to that in Huh7 cells, and was in clear contrast to the significantly lower titer in Hep3B/Cont cells (less than 10 FFU/ml). These results clearly indicate that expression of miR122 in Hep3B cells enables the establishment of a novel permissive cell line for the robust propagation of HCVcc.

Establishment of an HCV RNA replicon in Hep3B/miR122 cells. It has been shown that "cured" cells established through the elimination of the HCV genome from replicon cells by treatment with IFN-α exhibited more potent propagation of HCVcc than the original Huh7 cells (4). To establish a cured cell line derived from Hep3B/miR122 cells for further improvement of HCVcc propagation, we first established HCV replicon cells in Hep3B/miR122 cells. In vitro-transcribed sub- or full-genomic HCV RNA of the JFH1 strain was electroporated into Hep3B/miR122 and

4 2
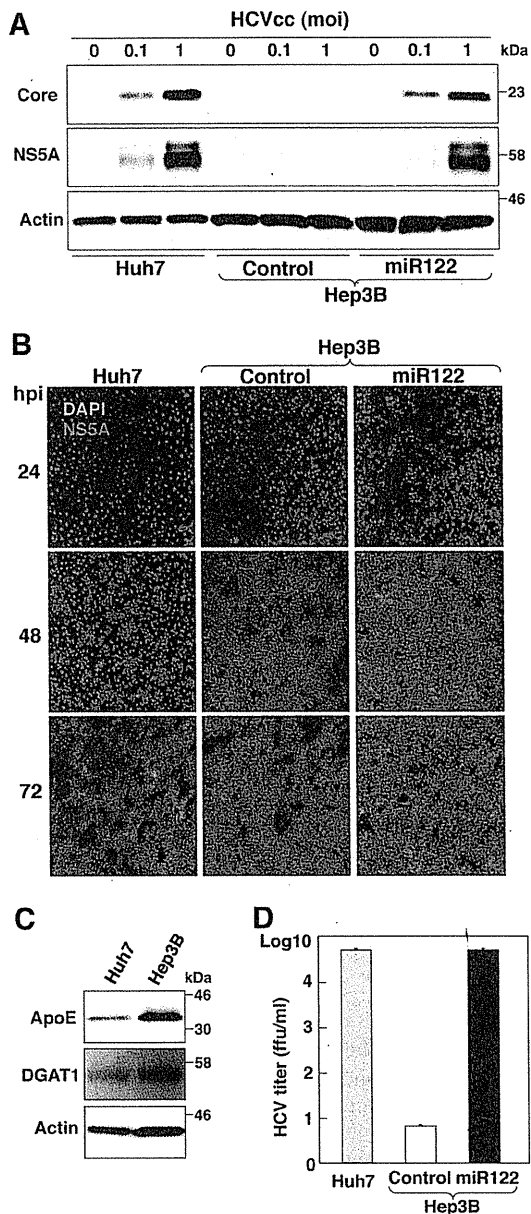
FIG 3 Establishment of a novel permissive cell line for robust propagation of HCVcc by expression of miR122 in Hep3B cells. (A) Huh7, Hep3B/Cont, and Hep3B/miR122 cells were infected with HCVcc at an MOI of 0.1 or 1, and the levels of expression of viral proteins were determined by immunoblotting using appropriate antibodies at 72 h postinfection. (B) Huh7, Hep3B/Cont, and Hep3B/miR122 cells were infected with HCVcc at an MOI of 1 and incubated with 1% methylcellulose in DMEM containing 5% FCS for the indicated time. Cells were fixed with 4% paraformaldehyde and subjected to indirect immunofluorescence assay using anti-NS5A antibody, followed by AF594-conjugated anti-rabbit IgG (red). Cell nuclei were stained with 4′,6-diamidino-2-phenylindole (DAPI; blue). (C) Huh7 and Hep3B cells were lysed and subjected to immunoblotting using appropriate antibodies. (D) Huh7, Hep3B/Cont, and Hep3B/miR122 cells were infected with HCVcc at an MOI of 1, the culture supernatants were collected at 72 h postinfection, and the viral titers of the supernatants were determined by focus-forming assay using Huh7.5.1 cells.

Hep3B/Cont cells, the cells were cultured with 400 μg/ml of G418 for 1 month, and subgenomic replicon (SGR) and full-genomic replicon (FGR) cells were established. Hep3B/miR122 cells electroporated with viral RNA generated a large number of colonies, in contrast to the complete absence of colony formation in Hep3B/Cont cells (Fig. 4A). High levels of HCV RNA comparable to those in the Huh7 cells harboring SGR of the JFH1 strain were detected in Hep3B/miR122 cells harboring either SGR or FGR of the JFH1 strain (Fig. 4B, lower). Expression of NS5A was detected in all of the clones of Hep3B/miR122 cells harboring either SGR or FGR, and that of the core protein was detected in all of the FGR clones (Fig. 4B, upper). HCV core protein and RNA were shown to localize mainly on the lipid droplets and on the cytoplasmic face of ER, respectively (40, 61). Immunofluorescence analyses revealed that dsRNA was colocalized with calnexin, an ER marker, in both SGR and FGR cells and HCV core protein was colocalized with lipid droplets in the FGR cells, as previously described (Fig. 4C). Treatment of Hep3B/miR122 cells harboring an FGR of the JFH1 strain with either CsA or IFN-α decreased the expression of core protein in a dose-dependent manner (Fig. 4D), suggesting that the Hep3B/miR122 replicon cells can be used for screening antiviral compounds for HCV.

Elimination of HCV RNA from HCV replicon RNA from Hep3B/miR122 cells enhances propagation of HCVcc. To establish cured Hep3B/miR122 cells, five clones of the Hep3B/miR122 replicon cells harboring FGR of the JFH1 strain were treated with 100 IU/ml of IFN-α to eliminate viral RNA, and viral RNA was gradually decreased and completely eliminated at 20 days posttreatment (Fig. 5A, left). We then examined the sensitivity of the cured cell clones for propagation of HCVcc. All of the cured cell clones exhibited enhancement of propagation of HCVcc, especially clone 5, which achieved a level of replication of HCVcc more than 6-fold higher than that in the parental Hep3B/miR122 cells (Fig. 5A, right). To examine the effect of serial passage of HCVcc in the cured Hep3B/miR122 cells, HCVcc was inoculated into the cured cells at an MOI of 0.1, and the culture supernatants harvested at 4 days postinfection were reinoculated into the naïve cured cells (Fig. 5B). Infectious titers in the culture supernatants were continuously increased in accord with the number of passages (Fig. 5C). These results indicate that a novel cell line capable of complete propagation of HCVcc was established by the introduction of miR122 and the curing process, as in the case of Huh7 cells by using Hep3B cells.

Cured Hep3B/miR122 cells facilitate efficient propagation of HCVcc through enhanced expression of miR122. It has been reported that one of the reasons for the high susceptibility of the cured cell line Huh7.5 to the propagation of HCVcc is the disruption of the innate immune responses caused by mutation in RIG-I, a key sensor for viral RNA in the cytoplasm (57, 69). To examine the innate immune response in the cured Hep3B/miR122 cells, reporter plasmids encoding the luciferase gene under the control of either the IFN-β (Fig. 6A, left) or ISRE (Fig. 6A, right) promoter were transfected into the cured or parental Hep3B/miR122 cells and stimulated with poly(I·C), VSV, or IFN-α. Activation of these promoters in the cured Hep3B/miR122 cells was not impaired but rather was enhanced upon stimulation with poly(I·C) or VSV compared with that in the parental cells. To further assess the authenticity of viral RNA recognition and ISG induction pathways in the cured Hep3B/miR122 cells, nuclear localization of IRF3 and STAT2 upon stimulation was determined by immuno-
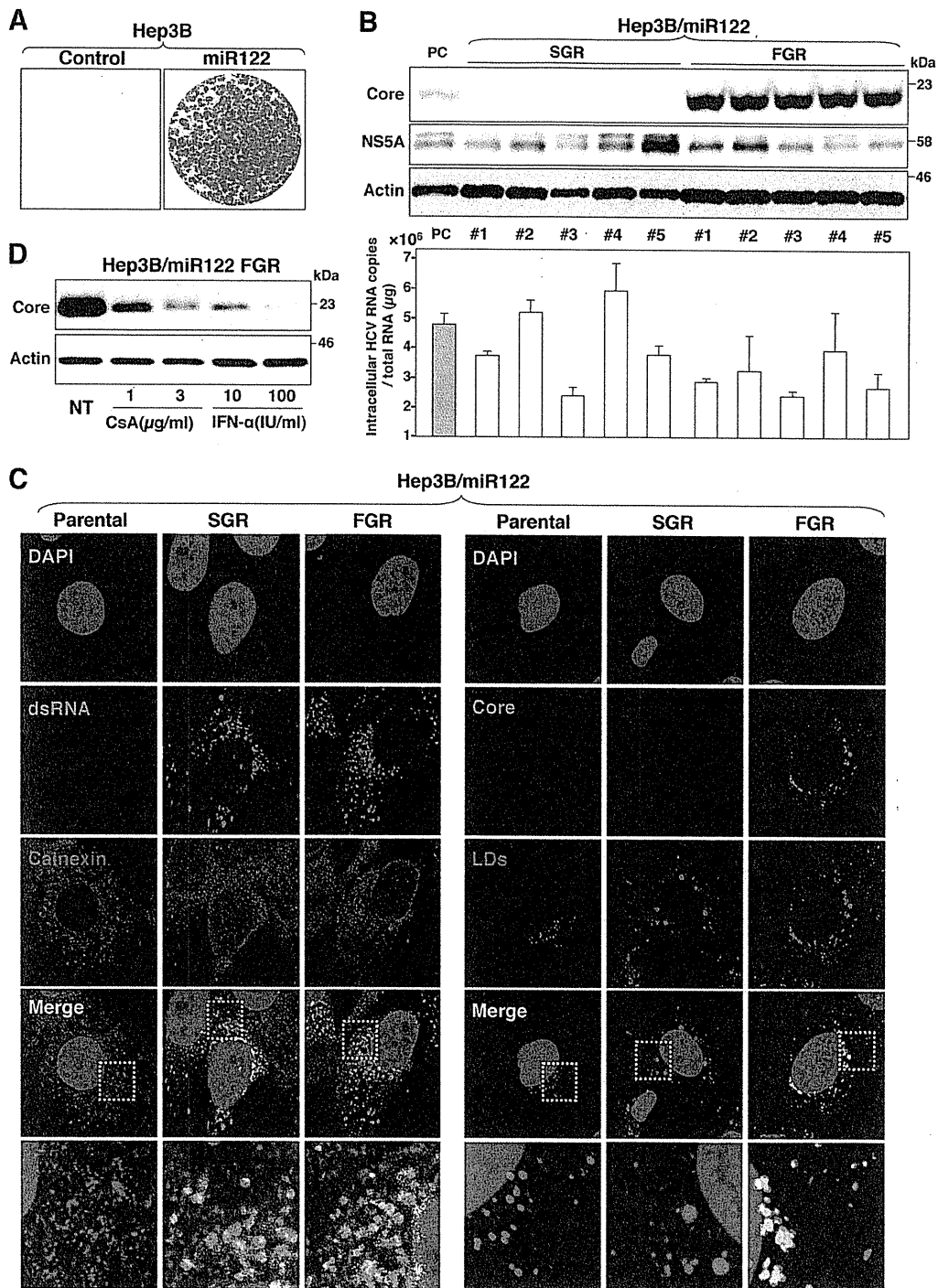
FIG 4 Establishment of an HCV RNA replicon in Hep3B/miR122 cells. (A) Full-genomic replicon RNA of HCV was electroporated into Hep3B/Cont and Hep3B/miR122 cells, and the medium was replaced with DMEM containing 10% FCS and 400 μg/ml G418 at 24 h posttransfection. Colony formation was determined as indicated in Materials and Methods. (B) (Upper) Sub- and full-genomic HCV replicons (SGR and FGR) in Hep3B/miR122 cells were subjected to immunoblotting using the appropriate antibodies. Huh7.5.1 cells infected with HCVcc were used as a positive control (PC). (Lower) Intracellular HCV copy number in replicon clones. SGR in Huh7 cells was used as a positive control. (C) SGR and FGR in Hep3B/miR122 cells were fixed with 4% paraformaldehyde and subjected to indirect immunofluorescence assay using the appropriate antibodies. Lipid droplets (LDs) were stained red with BODIPY. Cell nuclei were stained with 4′,6-diamidino-2-phenylindole (blue). The boxed regions in the merged images are magnified. (D) Hep3B/miR122 FGR cells were treated with DMEM containing 10% FCS and the indicated concentrations of CsA and IFN-α and then subjected to immunoblotting using appropriate antibodies at 48 h posttransfection. NT, no treatment.
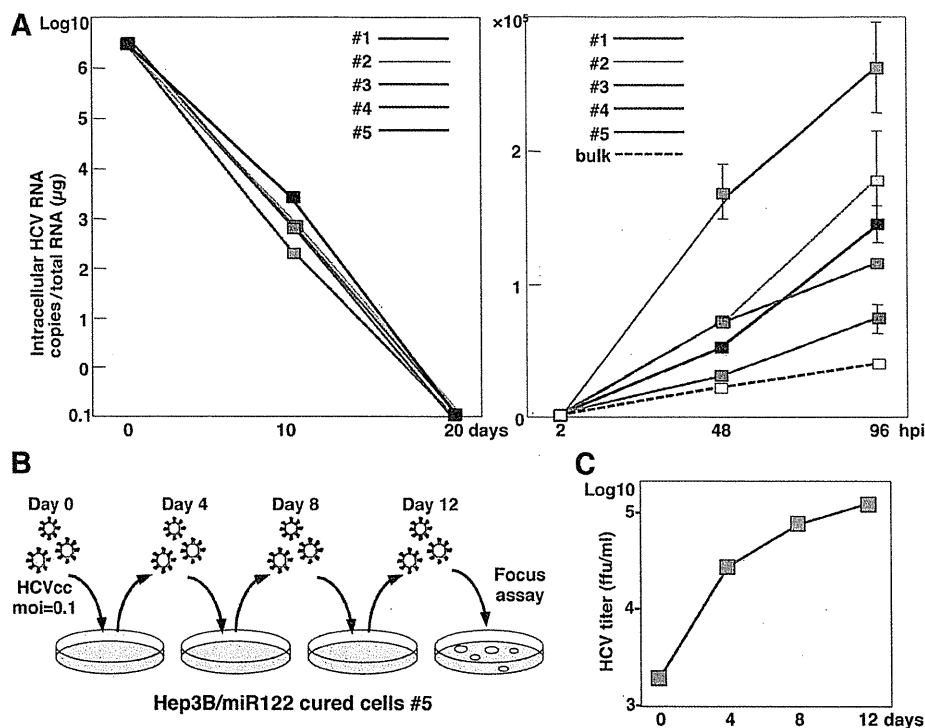
FIG 5 Elimination of HCV RNA from HCV replicon RNA from Hep3B/miR122 cells enhances propagation of HCVcc. (A) (Left) Hep3B/miR122 FGR cell clones were treated with IFN-α (100 IU/ml), and HCV RNA was determined by qRT-PCR at 10 and 20 days posttreatment; (right) Hep3B/miR122 parental cells (bulk) and the cured cells were infected with HCVcc at an MOI of 0.1, and HCV RNA was determined by qRT-PCR at 48 and 96 h postinfection. (B) Schematic diagram of the experimental procedure for serial passage of HCVcc in Hep3B/miR122 cured cells. The cured cells were infected with HCVcc at an MOI of 0.1. (C) The infectious titers in the culture supernatants of the Hep3B/miR122 cured cells were determined at the indicated time points by focus-forming assay using Hep3B/miR122 cells.
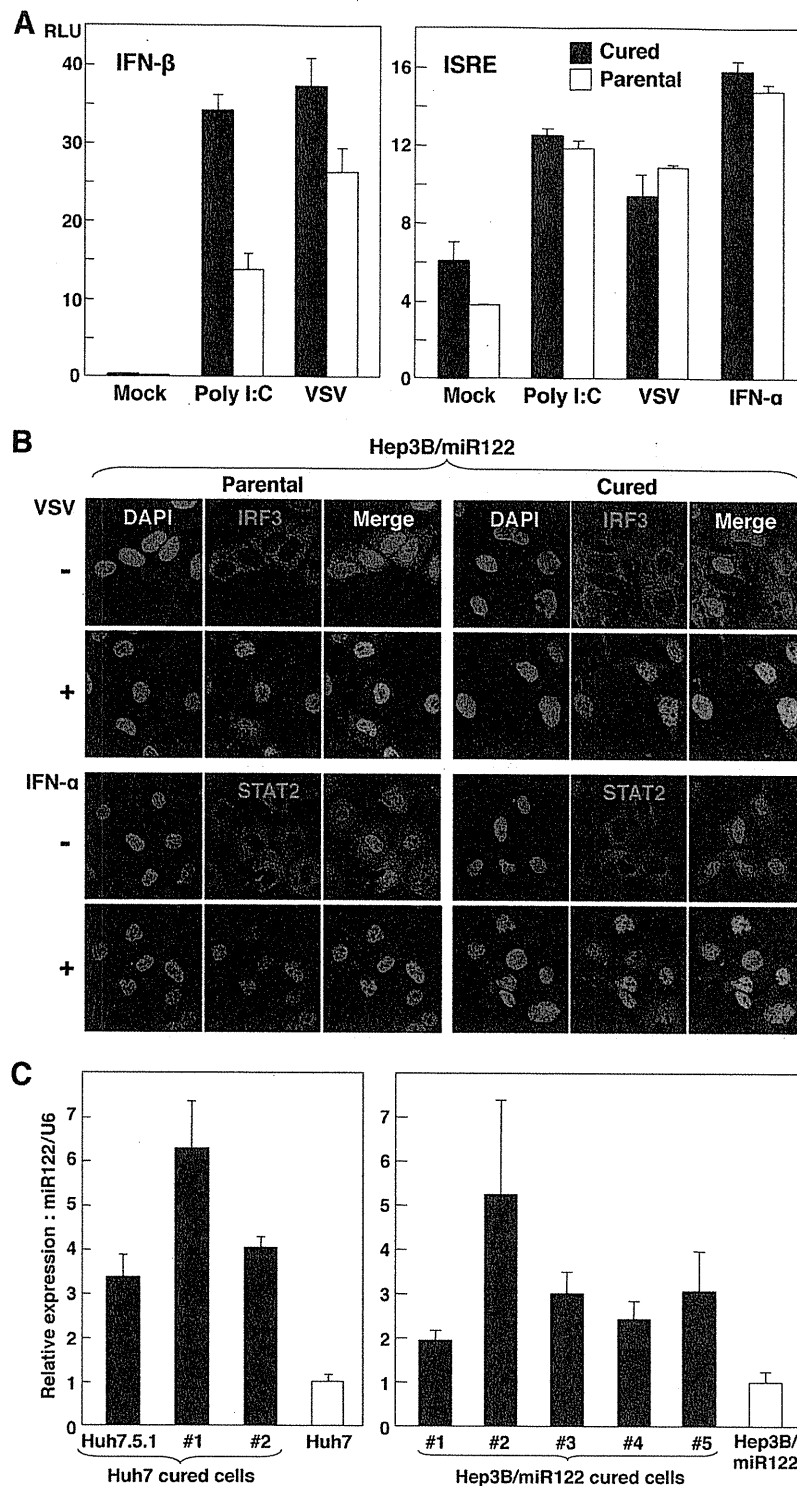
fluorescence analysis. IRF3 and STAT2 in both cured and parental Hep3B/miR122 cells were translocated into the nucleus upon stimulation with VSV and IFN-α, respectively (Fig. 6B). These results suggest that the efficient propagation of HCVcc in the cured Hep3B/miR122 cells might be attributable to reasons other than impairment of the innate immune response. Therefore, we hypothesized that the Hep3B/miR122 cells harboring the HCV genome are capable of surviving in the presence of a high concentration of G418 by amplification of the viral genome through enhancement of miR122 expression and that once HCV RNA was eliminated, the cured cells would acquire the ability to propagate HCV due to the high expression of miR122. To test this hypothesis, the levels of miR122 in both Huh7- and Hep3B/miR122-derived cured cells were compared with those in the parental cells. Intriguingly, both cured cell lines exhibited a significant increase of miR122 expression (approximately 2- to 6-fold) in comparison with that in the parental cells (Fig. 6C). These results suggest that the efficient propagation of HCVcc in the cured Hep3B/miR122 cells was partially attributable to an enhanced expression of miR122, rather than an impairment of the signaling pathway of innate immunity.

Specific interaction of miR122 with viral RNA is crucial for efficient propagation of HCVcc. To evaluate the effect of a specific interaction of miR122 with the target sequence in the 5′ UTR of HCV RNA on the enhancement of viral propagation, we generated two mutant pre-miR122s: sMT-miR122 has a substitution of uridine to adenosine, and dMT-miR122 carries an additional complementary substitution of adenosine to uridine to stabilize the expression. These substitutions have been shown to abrogate interaction with the target sequence (27) (Fig. 7A). A high level of expression of dMT-miR122 comparable to that of WT-miR122 was detected in Hep3B cells, in contrast to the low level of expression of sMT-miR122 (Fig. 7B). As described above, the expression level of miR122 in Hep3B cells was significantly lower than that in Huh7 cells (Fig. 1B). Taking advantage of this low level of miR122 expression, WT-miR122 and dMT-miR122 were exogenously expressed in Hep3B cells by the lentiviral vector to assess the importance of the specific interaction of miR122 with viral RNA. Not only intracellular viral RNA levels but also infectious titers in the culture supernatants were enhanced by the expression of WT-miR122, but they were not enhanced by the expression of dMT-miR122 (Fig. 7C and D). These results suggest that specific interaction of miR122 with the 5′ UTR of HCV is crucial for the efficient replication and propagation of HCV.

DISCUSSION

Most miRNAs utilize the normal RNA interfering pathway and repress translation of the target mRNAs (3, 26). For instance, miR122 targets the 3′ UTR of the cytoplasmic polyadenylation element binding protein (CPEB) (5), hemochromatosis (*Hfe*) and hemojuvelin (*Hjv*) (6), a disintegrin and metalloprotease family 10 (ADAM10) (2), and cationic amino transporter 1 (CAT-1) (8) and represses their translation. In contrast, HCV uniquely exploits the liver-specific miR122 to stimulate viral translation (23, 27–29,

A

IFN-β — RLU, y-axis: 40, 30, 20, 10, 0; x-axis: Mock, Poly I:C, VSV

ISRE — y-axis: 16, 12, 8, 4, 0; x-axis: Mock, Poly I:C, VSV, IFN-α

Legend: ■ Cured □ Parental

B

Hep3B/miR122

Parental | Cured

VSV — DAPI, IRF3, Merge | DAPI, IRF3, Merge
 (−)
 (+)

IFN-α — STAT2 | STAT2
 (−)
 (+)

C

Relative expression : miR122/U6 — y-axis: 7, 6, 5, 4, 3, 2, 1, 0

Left plot x-axis: Huh7.5.1, #1, #2 | Huh7 ; Huh7 cured cells

Right plot x-axis: #1, #2, #3, #4, #5 | Hep3B/miR122 ; Hep3B/miR122 cured cells

FIG 6 Cured Hep3B/miR122 cells facilitate efficient propagation of HCVcc through enhanced expression of miR122. (A) (Left) Hep3B/miR122 parental cells and cured cells of clone 5 were cotransfected with pIFNβ-Luc and pRL-TK and then infected with the VSV NCP mutant at an MOI of 0.01 or transfected with 1 μg of poly(I·C) at 24 h posttransfection, and luciferase activities were determined at 48 h posttreatment; (right) the cells were cotransfected with pISRE-Luc and pRL-TK and then infected with VSV at an MOI of 0.01 or treated with IFN-α (100 IU/ml) at 24 h posttransfection, and luciferase activities were determined at 48 h posttreatment. (B) (Upper) Hep3B/miR122 parental cells and the cured cells were infected with VSV at an MOI of 0.01, fixed with 4% phosphonoformic acid at 18 h postinfection, and subjected to indirect immunofluorescence assay using rabbit anti-IRF3 antibody, followed by AF488-conjugated anti-rabbit IgG (red); (lower) the cells were treated with IFN-α (100 IU/ml), fixed with 4% paraformaldehyde at 1 h postinfection, and subjected to indirect immunofluorescence assay using rabbit anti-STAT2 antibody, followed by AF488-conjugated anti-rabbit IgG (red). Cell nuclei were stained with 4′,6-diamidino-2-phenylindole (blue). (C) Total RNA was extracted from parental Huh7 and Hep3B/miR122 cells and their cured cells, and the relative expression of miR122 was determined by qRT-PCR by using U6 snRNA as an internal control.

4 6
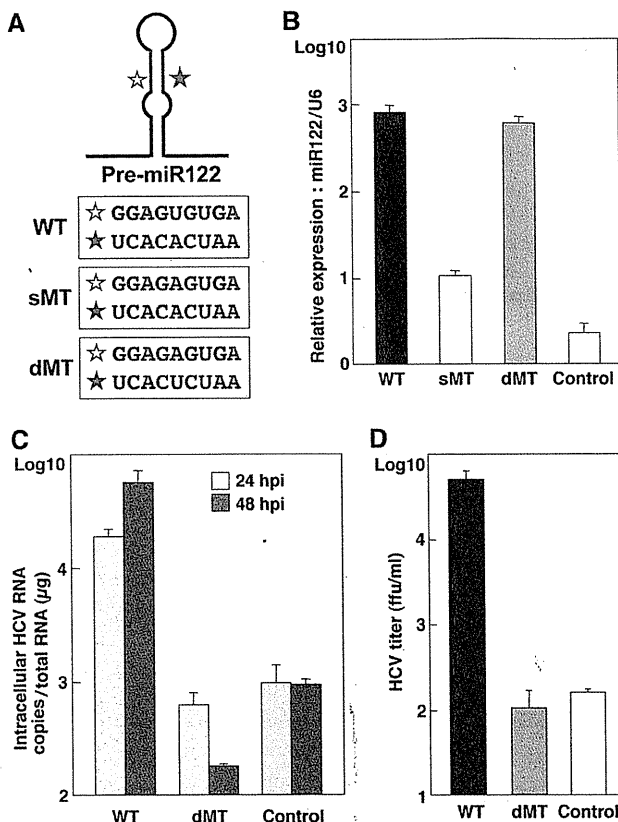
FIG 7 Specific interaction of miR122 with viral RNA is crucial for efficient propagation of HCVcc. (A) Diagram of pre-miR122 and partial nucleotide sequences of wild type (WT) miR122 and mutant miR122 carrying a single mutation (sMT) and double mutations (dMT). (B) Hep3B cells were transduced with lentiviral vectors expressing either WT-, sMT-, or dMT-miR122 or with a control, and the relative expression of miR122 was determined by qRT-PCR by using U6 snRNA as an internal control. (C) Hep3B cells expressing WT- or dMT-miR122 or the control cells were infected with HCVcc at an MOI of 1, and the level of HCV RNA was determined by qRT-PCR at 24 and 48 h postinfection. (D) The culture supernatants were collected at 72 h postinfection, and the viral titers of the supernatants were determined by focus-forming assay using Huh7.5.1 cells.

homogeneous population. This selection of certain clones is mainly caused by the host factors required for viral replication and immune pressure in a new host and is involved in the early phase of HCV infection in the new environment (18, 25, 32). A sole cell line, Huh7, has been employed in most of the experiments for *in vitro* studies of entry, RNA replication, and particle formation of HCV. Therefore, it has not been possible to assess propagation of HCVcc in human liver cell lines other than Huh7 cells and transmission of HCVcc to liver cell lines of different origins. The establishment of a novel human liver cell line, Hep3B/miR122, for propagation of HCVcc would help to generate new insights into the mutual interaction between HCV and human hepatocytes. Although we are not able to evaluate the effects of the acquired immunity on the induction of the adaptive mutations in cell culture systems, we can assess the host factors involved in the generation of the adaptive mutations by using two different human liver cell lines that support continuous propagation of HCVcc. Further studies are needed to determine the adaptive mutations in the HCV genome by passage in either Hep3B/miR122 or Huh7 cells and in one after the other.

At least seven major HCV genotypes and numerous subtypes have been identified (21), but laboratory strains capable of replicating *in vitro* are limited (36, 64, 68, 70). It is important to establish cell lines that permit the complete propagation of a wide range of HCV genotypes for further understanding of the life cycle of HCV. Although the partial replication of serum-derived HCV in primary hepatocytes in a specialized culture system has been reported (50), development of a simpler and more user-friendly system is required for promotion of research on HCV. It might be feasible to establish new cell culture systems for not only various genotypes of infectious HCV clones but also serum-derived HCV by the expression of miR122 in various human liver cell lines.

While preparing the manuscript, Narbus et al. reported that the expression of miR122 enhances HCV replication in HepG2/CD81 cells (46). Our data also demonstrated that the expression of miR122 increased HCV replication in HepG2/CD81 cells, as shown in Fig. 1D. However, the impact of miR122 expression on the production of infectious particles in HepG2/CD81 cells is significantly lower than that in Huh7 cells (46). Although LH86 (71) and Li23 (30) cell lines derived from human hepatocellular carcinoma have been shown to permit propagation of HCVcc, these cell lines are not well characterized. In contrast, the Hep3B cell line has been utilized in a wide range of research fields for a long time, resulting in the accumulation of many sources of data from genomic and proteomic analyses (1, 47, 55, 63, 67). Moreover, the Hep3B cell line is available from the major cell banks all over the world, which should readily allow reevaluation of the findings in this study. Comparison of the experimental data on HCVcc propagation between Huh7 and Hep3B/miR122 cells might provide a clue to understanding the host factors crucial for the efficient propagation of HCV in human liver cells.

The higher susceptibility to HCVcc propagation of the cured cells derived from Huh7 cells than the parental cells was suggested to be attributable to impairment of the innate immune response (57). However, this is not the only reason for efficient propagation of HCVcc in the Huh7-based cured cell lines (17). It has been shown that cured cell lines, such as Huh7.5.1 and Huh7-Lunet, express a higher level of miR122 than the parental Huh7 cells (13), suggesting that upregulation of miR122 in the cured cells participates in the efficient propagation of HCVcc. However, the level of

38, 52). In this study, we assessed the possibility of establishment of human liver cell lines that are susceptible to HCVcc propagation through exogenous expression of miR122 by a lentiviral vector. Although Huh7 cells and their derived cell lines are highly susceptible to propagation of HCVcc, they intrinsically express an abundant amount of miR122. Among the cell lines that we investigated, Hep3B cells exhibit a high sensitivity to HCVcc propagation by expression of miR122 compared to that of Huh7 cells, whereas no sensitivity to HCVcc was observed in the parental Hep3B cells. Therefore, the Hep3B cell line was suggested to be an ideal tool to investigate miR122 function in the life cycle of HCV.

RNA viruses replicate in host cells with high error rates, generating a broad population diversity, which allows rapid adaptation to new environments (33). HCV propagates in the liver of patients with quasispecies heterogeneity and transmits to a new host through contaminated blood or blood products (16). It is known that the complexity of HCV clones significantly decreases during transmission through a genetic bottleneck, resulting in a more

miR122 expression in the cured Hep3B cells was not necessarily correlated with the replication efficiency of HCVcc in the present work (Fig. 6C). Most recently, Denard et al. reported that the expression of CREB3L1/OASIS, which specifically prevents division of virus-infected cells, in cured Huh7 cells was reduced compared to that in the parental cells (12), suggesting that CREB3L1/OASIS is also involved in the enhancement of HCVcc propagation in the cured cells.

In this study, we have shown that expression of miR122 confers susceptibility to human liver cell lines for the efficient propagation of HCVcc. Elimination of the HCV genome from the replicon cells of Hep3B/miR122 cells enhanced propagation of HCVcc in accord with the increment of miR122 expression, and propagation of HCVcc in the cured cells was continuously increased in every passage. Furthermore, the interaction between HCV RNA and miR122 was shown to be specific for production of infectious particles in Hep3B/miR122 cells. The establishment of a new permissive cell line for HCVcc allows us not only to investigate the biological function of miR122 on the life cycle of HCV but also to develop novel therapeutics for chronic hepatitis C.

ACKNOWLEDGMENTS

REFERENCES

1. Aden DP, Fogel A, Plotkin S, Damjanov I, Knowles BB. 1979. Controlled synthesis of HBsAg in a differentiated human liver carcinoma-derived cell line. Nature 282:615–616.
2. Bai S, et al. 2009. MicroRNA-122 inhibits tumorigenic properties of hepatocellular carcinoma cells and sensitizes these cells to sorafenib. J. Biol. Chem. 284:32015–32027.
3. Bartel DP. 2009. MicroRNAs: target recognition and regulatory functions. Cell 136:215–233.
4. Blight KJ, McKeating JA, Rice CM. 2002. Highly permissive cell lines for subgenomic and genomic hepatitis C virus RNA replication. J. Virol. 76: 13001–13014.
5. Burns DM, D'Ambrogio A, Nottrott S, Richter JD. 2011. CPEB and two poly(A) polymerases control miR-122 stability and p53 mRNA translation. Nature 473:105–108.
6. Castoldi M, et al. 2011. The liver-specific microRNA miR-122 controls systemic iron homeostasis in mice. J. Clin. Invest. 121:1386–1396.
7. Chang J, et al. 2008. Liver-specific microRNA miR-122 enhances the replication of hepatitis C virus in nonhepatic cells. J. Virol. 82:8215–8223.
8. Chang J, et al. 2004. miR-122, a mammalian liver-specific microRNA, is processed from hcr mRNA and may downregulate the high affinity cationic amino acid transporter CAT-1. RNA Biol. 1:106–113.
9. Chang KS, Jiang J, Cai Z, Luo G. 2007. Human apolipoprotein E is required for infectivity and production of hepatitis C virus in cell culture. J. Virol. 81:13783–13793.
10. Cormier EG, et al. 2004. CD81 is an entry coreceptor for hepatitis C virus. Proc. Natl. Acad. Sci. U. S. A. 101:7270–7274.
11. Date T, et al. 2004. Genotype 2a hepatitis C virus subgenomic replicon can replicate in HepG2 and IMY-N9 cells. J. Biol. Chem. 279: 22371–22376.
12. Denard B, et al. 2011. The membrane-bound transcription factor CREB3L1 is activated in response to virus infection to inhibit proliferation of virus-infected cells. Cell Host Microbe 10:65–74.
13. Ehrhardt M, et al. 18 April 2011. Profound differences of microRNA expression patterns in hepatocytes and hepatoma cell lines commonly used in hepatitis C virus studies. Hepatology. [Epub ahead of print.]
14. Elmen J, et al. 2008. LNA-mediated microRNA silencing in non-human primates. Nature 452:896–899.
15. Evans MJ, et al. 2007. Claudin-1 is a hepatitis C virus co-receptor required for a late step in entry. Nature 446:801–805.
16. Farci P, et al. 2000. The outcome of acute hepatitis C predicted by the evolution of the viral quasispecies. Science 288:339–344.
17. Feigelstock DA, Mihalik KB, Kaplan G, Feinstone SM. 2010. Increased susceptibility of Huh7 cells to HCV replication does not require mutations in RIG-I. Virol. J. 7:44.
18. Feliu A, Gay E, Garcia-Retortillo M, Saiz JC, Forns X. 2004. Evolution of hepatitis C virus quasispecies immediately following liver transplantation. Liver Transpl. 10:1131–1139.
19. Ge D, et al. 2009. Genetic variation in IL28B predicts hepatitis C treatment-induced viral clearance. Nature 461:399–401.
20. Gentzsch J, et al. 2011. Hepatitis C virus complete life cycle screen for identification of small molecules with pro- or antiviral activity. Antiviral Res. 89:136–148.
21. Gottwein JM, et al. 2009. Development and characterization of hepatitis C virus genotype 1-7 cell culture systems: role of CD81 and scavenger receptor class B type I and effect of antiviral drugs. Hepatology 49: 364–377.
22. Haid S, Windisch MP, Bartenschlager R, Pietschmann T. 2010. Mouse-specific residues of claudin-1 limit hepatitis C virus genotype 2a infection in a human hepatocyte cell line. J. Virol. 84:964–975.
23. Henke JI, et al. 2008. microRNA-122 stimulates translation of hepatitis C virus RNA. EMBO J. 27:3300–3310.
24. Herker E, et al. 2010. Efficient hepatitis C virus particle formation requires diacylglycerol acyltransferase-1. Nat. Med. 16:1295–1298.
25. Hughes MG, Jr, et al. 2005. HCV infection of the transplanted liver: changing CD81 and HVR1 variants immediately after liver transplantation. Am. J. Transplant. 5:2504–2513.
26. Huntzinger E, Izaurralde E. 2011. Gene silencing by microRNAs: contributions of translational repression and mRNA decay. Nat. Rev. Genet. 12:99–110.
27. Jangra RK, Yi M, Lemon SM. 2010. Regulation of hepatitis C virus translation and infectious virus production by the microRNA miR-122. J. Virol. 84:6615–6625.
28. Jopling CL, Schutz S, Sarnow P. 2008. Position-dependent function for a tandem microRNA miR-122-binding site located in the hepatitis C virus RNA genome. Cell Host Microbe 4:77–85.
29. Jopling CL, Yi M, Lancaster AM, Lemon SM, Sarnow P. 2005. Modulation of hepatitis C virus RNA abundance by a liver-specific microRNA. Science 309:1577–1581.
30. Kato N, et al. 2009. Efficient replication systems for hepatitis C virus using a new human hepatoma cell line. Virus Res. 146:41–50.
31. Lanford RE, et al. 2010. Therapeutic silencing of microRNA-122 in primates with chronic hepatitis C virus infection. Science 327:198–201.
32. Laskus T, et al. 2004. Analysis of hepatitis C virus quasispecies transmission and evolution in patients infected through blood transfusion. Gastroenterology 127:764–776.
33. Lauring AS, Andino R. 2010. Quasispecies theory and the behavior of RNA viruses. PLoS Pathog. 6:e1001005.
34. Lavanchy D. 2009. The global burden of hepatitis C. Liver Int. 29(Suppl. 1):74–81.
35. Lin LT, et al. 2010. Replication of subgenomic hepatitis C virus replicons in mouse fibroblasts is facilitated by deletion of interferon regulatory factor 3 and expression of liver-specific microRNA 122. J. Virol. 84: 9170–9180.
36. Lindenbach BD, et al. 2005. Complete replication of hepatitis C virus in cell culture. Science 309:623–626.
37. Lohmann V, et al. 1999. Replication of subgenomic hepatitis C virus RNAs in a hepatoma cell line. Science 285:110–113.
38. Machlin ES, Sarnow P, Sagan SM. 2011. Masking the 5' terminal nucleotides of the hepatitis C virus genome by an unconventional microRNA-target RNA complex. Proc. Natl. Acad. Sci. U. S. A. 108:3193–3198.
39. Masaki T, et al. 2010. Production of infectious hepatitis C virus by using RNA polymerase I-mediated transcription. J. Virol. 84:5824–5835.
40. Miyanari Y, et al. 2007. The lipid droplet is an important organelle for hepatitis C virus production. Nat. Cell Biol. 9:1089–1097.
41. Moradpour D, Penin F, Rice CM. 2007. Replication of hepatitis C virus. Nat. Rev. Microbiol. 5:453–463.
42. Moriishi K, Matsuura Y. 2007. Evaluation systems for anti-HCV drugs. Adv. Drug Deliv. Rev. 59:1213–1221.

4 8

43. Moriishi K, Matsuura Y. 2007. Host factors involved in the replication of hepatitis C virus. Rev. Med. Virol. 17:343–354.
44. Moriishi K, Matsuura Y. 2003. Mechanisms of hepatitis C virus infection. Antivir. Chem. Chemother. 14:285–297.
45. Moriishi K, et al. 2010. Involvement of PA28gamma in the propagation of hepatitis C virus. Hepatology 52:411–420.
46. Narbus CM, et al. 2011. HepG2 cells expressing microRNA miR-122 support the entire hepatitis C virus life cycle. J. Virol. 85:12087–12092.
47. Park JG, et al. 1995. Characterization of cell lines established from human hepatocellular carcinoma. Int. J. Cancer 62:276–282.
48. Pileri P, et al. 1998. Binding of hepatitis C virus to CD81. Science 282: 938–941.
49. Ploss A, et al. 2009. Human occludin is a hepatitis C virus entry factor required for infection of mouse cells. Nature 457:882–886.
50. Ploss A, et al. 2010. Persistent hepatitis C virus infection in microscale primary human hepatocyte cultures. Proc. Natl. Acad. Sci. U. S. A. 107: 3141–3145.
51. Randall G, et al. 2007. Cellular cofactors affecting hepatitis C virus infection and replication. Proc. Natl. Acad. Sci. U. S. A. 104:12884–12889.
52. Roberts AP, Lewis AP, Jopling CL. 2011. miR-122 activates hepatitis C virus translation by a specialized mechanism requiring particular RNA components. Nucleic Acids Res. 39:7716–7729.
53. Russell RS, et al. 2008. Advantages of a single-cycle production assay to study cell culture-adaptive mutations of hepatitis C virus. Proc. Natl. Acad. Sci. U. S. A. 105:4370–4375.
54. Scarselli E, et al. 2002. The human scavenger receptor class B type I is a novel candidate receptor for the hepatitis C virus. EMBO J. 21:5017–5025.
55. Seow TK, Liang RC, Leow CK, Chung MC. 2001. Hepatocellular carcinoma: from bedside to proteomics. Proteomics 1:1249–1263.
56. Skalsky RL, Cullen BR. 2010. Viruses, microRNAs, and host interactions. Annu. Rev. Microbiol. 64:123–141.
57. Sumpter R, Jr, et al. 2005. Regulating intracellular antiviral defense and permissiveness to hepatitis C virus RNA replication through a cellular RNA helicase, RIG-I. J. Virol. 79:2689–2699.
58. Suppiah V, et al. 2009. IL28B is associated with response to chronic hepatitis C interferon-alpha and ribavirin therapy. Nat. Genet. 41: 1100–1104.
59. Tanaka Y, et al. 2009. Genome-wide association of IL28B with response to pegylated interferon-alpha and ribavirin therapy for chronic hepatitis C. Nat. Genet. 41:1105–1109.
60. Tani H, et al. 2007. Replication-competent recombinant vesicular stomatitis virus encoding hepatitis C virus envelope proteins. J. Virol. 81: 8601–8612.
61. Targett-Adams P, Boulant S, McLauchlan J. 2008. Visualization of double-stranded RNA in cells supporting hepatitis C virus RNA replication. J. Virol. 82:2182–2195.
62. Thomas DL, et al. 2009. Genetic variation in IL28B and spontaneous clearance of hepatitis C virus. Nature 461:798–801.
63. Vannucchi AM, et al. 1993. Effects of cyclosporin A on erythropoietin production by the human Hep3B hepatoma cell line. Blood 82:978–984.
64. Wakita T, et al. 2005. Production of infectious hepatitis C virus in tissue culture from a cloned viral genome. Nat. Med. 11:791–796.
65. Walters KA, et al. 2006. Host-specific response to HCV infection in the chimeric SCID-beige/Alb-uPA mouse model: role of the innate antiviral immune response. PLoS Pathog. 2:e59.
66. Windisch MP, et al. 2005. Dissecting the interferon-induced inhibition of hepatitis C virus replication by using a novel host cell line. J. Virol. 79: 13778–13793.
67. Wong N, et al. 2005. Transcriptional profiling identifies gene expression changes associated with IFN-alpha tolerance in hepatitis C-related hepatocellular carcinoma cells. Clin. Cancer Res. 11:1319–1326.
68. Yi M, Villanueva RA, Thomas DL, Wakita T, Lemon SM. 2006. Production of infectious genotype 1a hepatitis C virus (Hutchinson strain) in cultured human hepatoma cells. Proc. Natl. Acad. Sci. U. S. A. 103: 2310–2315.
69. Yoneyama M, et al. 2004. The RNA helicase RIG-I has an essential function in double-stranded RNA-induced innate antiviral responses. Nat. Immunol. 5:730–737.
70. Zhong J, et al. 2005. Robust hepatitis C virus infection in vitro. Proc. Natl. Acad. Sci. U. S. A. 102:9294–9299.
71. Zhu H, et al. 2007. Hepatitis C virus triggers apoptosis of a newly developed hepatoma cell line through antiviral defense system. Gastroenterology 133:1649–1659.

4 9

Vol. 85, No. 24

Dysfunction of Autophagy Participates in Vacuole Formation and Cell Death in Cells Replicating Hepatitis C Virus[▽][§]

Shuhei Taguwa,[1][†] Hiroto Kambara,[1][†] Naonobu Fujita,[2] Takeshi Noda,[2] Tamotsu Yoshimori,[2] Kazuhiko Koike,[3] Kohji Moriishi,[4] and Yoshiharu Matsuura[1]*

Department of Molecular Virology, Research Institute for Microbial Diseases,[1] and Department of Genetics, Graduate School of Medicine,[2] Osaka University, Osaka 565-0871, Department of Gastroenterology, Graduate School of Medicine, University of Tokyo, Tokyo 113-8655,[3] and Department of Microbiology, Faculty of Medicine, Yamanashi University, Yamanashi 409-3898,[4] Japan

Hepatitis C virus (HCV) is a major cause of chronic liver diseases. A high risk of chronicity is the major concern of HCV infection, since chronic HCV infection often leads to liver cirrhosis and hepatocellular carcinoma. Infection with the HCV genotype 1 in particular is considered a clinical risk factor for the development of hepatocellular carcinoma, although the molecular mechanisms of the pathogenesis are largely unknown. Autophagy is involved in the degradation of cellular organelles and the elimination of invasive microorganisms. In addition, disruption of autophagy often leads to several protein deposition diseases. Although recent reports suggest that HCV exploits the autophagy pathway for viral propagation, the biological significance of the autophagy to the life cycle of HCV is still uncertain. Here, we show that replication of HCV RNA induces autophagy to inhibit cell death. Cells harboring an HCV replicon RNA of genotype 1b strain Con1 but not of genotype 2a strain JFH1 exhibited an incomplete acidification of the autolysosome due to a lysosomal defect, leading to the enhanced secretion of immature cathepsin B. The suppression of autophagy in the Con1 HCV replicon cells induced severe cytoplasmic vacuolation and cell death. These results suggest that HCV harnesses autophagy to circumvent the harmful vacuole formation and to maintain a persistent infection. These findings reveal a unique survival strategy of HCV and provide new insights into the genotype-specific pathogenicity of HCV.

Hepatitis C virus (HCV) is a major causative agent of blood-borne hepatitis and currently infects at least 180 million people worldwide (58). The majority of individuals infected with HCV develop chronic hepatitis, which eventually leads to liver cirrhosis and hepatocellular carcinoma (25, 48). In addition, HCV infection is known to induce extrahepatic diseases such as type 2 diabetes and malignant lymphoma (20). It is believed that the frequency of development of these diseases varies among viral genotypes (14, 51). However, the precise mechanism of the genotype-dependent outcome of HCV-related diseases has not yet been elucidated. Despite HCV's status as a major public health problem, the current therapy with pegylated interferon and ribavirin is effective in only around 50% of patients with genotype 1, which is the most common genotype worldwide, and no effective vaccines for HCV are available (35, 52). Although recently approved protease inhibitors for HCV exhibited a potent antiviral efficacy in patients with genotype 1 (36, 43), the emergence of drug-resistant mutants is a growing problem (16). Therefore, it is important to clarify the life cycle and pathogenesis of HCV for the development of more potent remedies for chronic hepatitis C.

HCV belongs to the genus *Hepacivirus* of the family *Flaviviridae* and possesses a single positive-stranded RNA genome with a nucleotide length of 9.6 kb, which encodes a single polyprotein consisting of approximately 3,000 amino acids (40). The precursor polyprotein is processed by host and viral proteases into structural and nonstructural (NS) proteins (34). Not only viral proteins but also several host factors are required for efficient replication of the HCV genome, where NS5A is known to recruit various host proteins and to form replication complexes with other NS proteins (39). In the HCV-propagating cell, host intracellular membranes are reconstructed for the viral niche known as the membranous web, where it is thought that progeny viral RNA and proteins are concentrated for efficient replication and are protected from defensive degradation, as are the host protease and nucleases (38).

Autophagy is a bulk degradation process, wherein portions of cytoplasm and organelles are enclosed by a unique membrane structure called an autophagosome, which subsequently fuses with the lysosome for degradation (37, 60). Autophagy occurs not only in order to recycle amino acids during starvation but also to clear away deteriorated proteins or organelles irrespective of nutritional stress. In fact, the deficiency of autophagy leads to the accumulation of disordered proteins that can ultimately cause a diverse range of diseases, including neurodegeneration and liver injury (12, 29, 30), and often to type 2 diabetes and malignant lymphoma (9, 32).

Recently, it has been shown that autophagy is provoked upon replication of several RNA viruses and is closely related to their propagation and/or pathogenesis. Coxsackievirus B3

* Corresponding author. Mailing address: Department of Molecular Virology, Research Institute for Microbial Diseases, Osaka University, 3-1, Yamadaoka, Suita-shi, Osaka 565-0871, Japan. Phone: 81-6-6879-8340. Fax: 81-6-6879-8269. E-mail: matsuura@biken.osaka-u.ac.jp.
† These authors contributed equally to this work.
§ Supplemental material for this article may be found at http://jvi.asm.org/.
▽ Published ahead of print on 12 October 2011.

5 0

utilizes autophagic membrane as a site of genome replication, whereas influenza virus attenuates apoptosis through the induction of autophagy (10, 59). Moreover, several groups have reported that HCV induces autophagy for infection or replication (5, 49); however, the role(s) of autophagy in the propagation of HCV is still controversial and the involvement of autophagy in the pathogenesis of HCV has not yet been clarified. In this study, we examined the biological significance of the autophagy observed in cells in which the HCV genome replicates.

MATERIALS AND METHODS

Plasmids. The plasmids pmStrawberry-C1, pmStrawberry-Atg4B^{C74A}, pm-RFP-GFP-LC3, pEGFP-LC3, and pEGFP-Atg16L were described previously (7, 8, 24). The plasmids pFGR-JFH1 and pSGR-JFH1 were kind gifts from T. Wakita.

Cell culture. All cell lines were cultured at 37°C under a humidified atmosphere with 5% CO_2. Huh7 cells were cultivated in Dulbecco's modified Eagle's medium (DMEM) supplemented with 10% fetal bovine serum (FBS), nonessential amino acids, 100 U/ml penicillin, and 100 mg/ml streptomycin. For the starvation, the cells were cultivated with Earle's balanced salt solution (EBSS) (Sigma) for 6 h. HCV replicon cells were established as described previously (53). The plasmid pairs pFK-I$_{389}$ neo/NS3-3′/NK5.1 and pFK-I$_{389}$ neo/FGR/NK5.1 and pFGR-JFH1 and pSGR-JFH1 were linearized with ScaI or XbaI. The plasmids pFGR-JFH1 and pSGR-JFH1 were treated with mung bean exonuclease. The linearized DNA was transcribed in vitro by using the MEGAscript T7 kit (Applied Biosystems) according to the manufacturer's protocol. The transcribed RNA was electroporated into cells under conditions of 270 V and 960 mF using a Gene Pulser (Bio-Rad). All HCV replicon cells were maintained in DMEM containing 10% FBS, nonessential amino acids, and 1 mg/ml G418 (Nacalai).

Reagents and antibodies. Concanamycin A and bafilomycin A1 were purchased from Sigma and Fluka, respectively. E64D and pepstatin A were from Peptide Institute Inc. Rabbit anti-HCV NS5A polyclonal antibody was described previously (45). Mouse monoclonal anti-JEV NS3 antibody was prepared by immunization using the recombinant protein spanning amino acid residues 171 to 619 of JEV NS3. Rabbit polyclonal anti-LC3 (PM036), mouse monoclonal anti-RFP (8D6), and anti-62/SQSTM1 (5F2) antibodies were purchased from Medical & Biological Laboratories. Rabbit polyclonal anti-cathepsin B (FL-339) and mouse monoclonal anti-LAMP1 (H4A3) antibodies were from Santa Cruz Biotechnology. Mouse monoclonal anti-HCV NS5A (HCM-131-5), rabbit polyclonal anti-β-actin, and mouse monoclonal anti-Golgin97 (CDF4) antibodies were from Austral Biologicals, Sigma, and Invitrogen, respectively. Mouse monoclonal and rabbit polyclonal anti-cathepsin B antibodies were from Calbiochem. Mouse monoclonal anti-p62/SQSTM1 (5F2) and anti-ATP6V0D1 (ab56441) antibodies were from Abcam. Rabbit polyclonal anti-Atg4B antibody was from Sigma. Mouse anti-double-stranded RNA (dsRNA) IgG2a (J2 and K1) antibodies were from Biocenter Ltd. (Szirak, Hungary).

Transfection, infection, and immunoblotting. Transfection and infection were carried out as described previously (53). Each lysosome-enriched fraction was isolated by using the Lysosome Enrichment Kit for Tissue and Cultured Cells (Pierce) according to the manufacturer's protocol. Samples were subjected to 12.5% sodium dodecyl sulfate-polyacrylamide gel electrophoresis. The proteins were transferred to polyvinylidene difluoride membranes (Millipore) and were reacted with the appropriate antibodies. The immune complexes were visualized with Super Signal West Femto substrate (Pierce) and detected by an LAS-3000 image analyzer system (Fujifilm). The protein bands of LC3 and β-actin were quantified by Multi Gauge software (Fujifilm), and the values of LC3 were normalized to those of β-actin.

Fluorescence microscopy. Cells were cultured on glass slides and then fixed with 4% paraformaldehyde in phosphate-buffered saline (PBS) at room temperature for 30 min. After being washed twice with PBS, the cells were permeabilized at room temperature for 20 min with PBS containing 0.25% saponin and then blocked with PBS containing 0.2% gelatin (gelatin-PBS) for 60 min at room temperature. The cells were incubated with gelatin-PBS containing appropriate antibodies at 37°C for 60 min and washed three times with PBS containing 1% Tween 20 (PBST). The resulting cells were incubated with gelatin-PBS containing corresponding fluorescent-conjugated secondary antibodies at 37°C for 60 min and then washed three times with PBST. The stained cells were covered with Vectashield mounting medium containing DAPI (4′,6-diamidino-2-phenylin-

dole) (Vector Laboratories Inc.) and observed with a FluoView FV1000 laser scanning confocal microscope (Olympus). Time-lapse video microscopy was performed at 37°C with a DeltaVision microscope system (Applied Precision Inc.) equipped with a ΔTC3 culture dish system (Bioptechs) for temperature control.

Quantification of pro-cathepsin B. Each cell line was seeded on 12-well type I collagen-coated dishes (IWAKI) and cultured for 48 h. The supernatant and the cells were harvested and subjected to quantification of pro-cathepsin B by using Quantikine human pro-cathepsin B immunoassay (R&D Systems) according to the manufacturer's protocol.

Statistical analysis. Estimated values were represented as the means ± standard deviations. The significance of differences in the means was determined by Student's t test.

RESULTS

Autophagy is induced in the HCV replicating cell in a strain-dependent manner. To determine whether autophagy is induced during the replication of HCV, we investigated the phosphoethanolamine (PE) conjugation of LC3 in HCV replicon cells in which HCV RNA was autonomously replicating. As shown in Fig. 1A, the amounts of PE-conjugated LC-3 (LC3-II), a conventional marker for an autophagosomal membrane, in Huh7 cells were slightly increased by starvation, in conjunction with a reduction of the unmodified LC-3 (LC3-I). In contrast, the amount of LC3-II was significantly increased in the subgenomic and full genomic HCV replicon cells of the genotype 1b strain Con1 (SGR^{Con1} and FGR^{Con1}), whereas a small amount of LC3-II was detected in the full genomic replicon cells of the genotype 2a strain JFH1 (FGR^{JFH1}). We also examined the subcellular localization of LC3 by using confocal microscopy. Although LC3 was diffusely detected in the cytoplasm of naïve Huh7 cells, small foci of the accumulated LC3 appeared after starvation (Fig. 1B), whereas many LC3 foci that were larger in size than those in the starved cells appeared in the cytoplasm, particularly near the nucleus, in both SGR^{Con1} and FGR^{Con1} cells. However, a low level of LC3 focus formation comparable to that in the starved cells was observed in the FGR^{JFH1} cells. Most of the LC3 foci were not colocalized with NS5A, an HCV protein of the viral replication complex, in the HCV replicon cells, as reported previously (49). Elimination of HCV RNA from the SGR^{Con1} cells by treatment with alpha interferon (SGR^{cured}) abrogated the lipidation and accumulation of LC3 (Fig. 1C and D). Interestingly, overexpression of the HCV polyprotein of genotype 1b by an expression plasmid induced no autophagy (data not shown), suggesting that replication of viral RNA is required for induction of autophagy. Furthermore, neither lipidation nor accumulation of LC3 was observed in SGR^{JEV} cells harboring subgenomic replicon RNA cells of Japanese encephalitis virus (JEV), which is also a member of the family Flaviviridae (Fig. 1C and D). These results suggest that replication of HCV but not that of JEV induces autophagy.

The autophagy flux is impaired in the replicon cells of HCV strain Con1 after a step of autophagosome formation. To further examine the autophagy induced in the HCV replicon cells in more detail, Huh7 and SGR^{Con1} cells were treated with pepstatin A and E64D, inhibitors of aspartic protease and cysteine protease, respectively. In this assay, treatment of intact cells capable of inducing autophagy with the inhibitors increases the amount of LC3-II, whereas no increase is observed in cells impaired in the autophagic degradation. The amount of LC3-II was significantly increased in the naïve Huh7
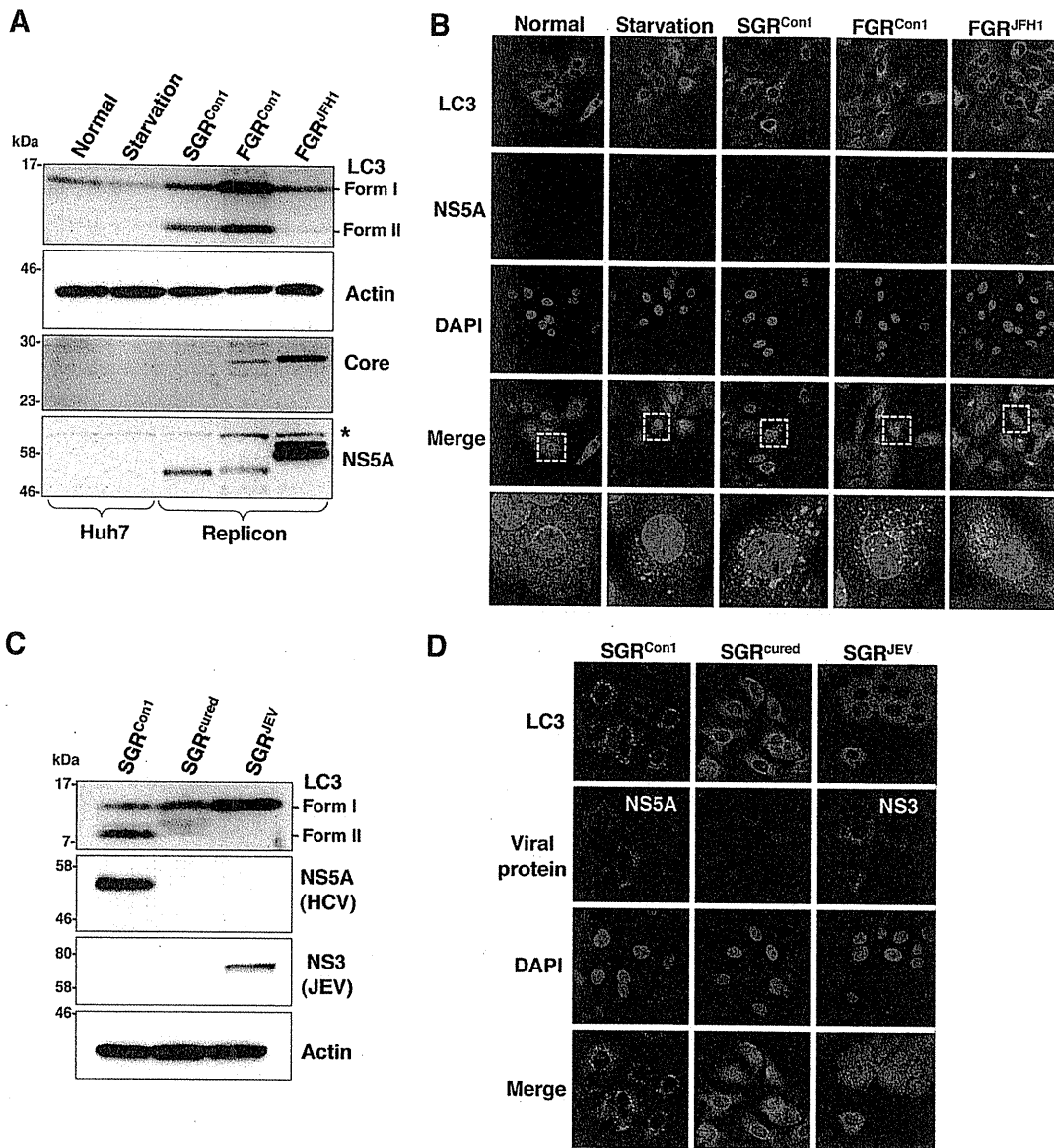
FIG. 1. Induction of autophagy in the HCV replicon cells. (A) The starved Huh7 cells and HCV replicon cells harboring a sub- or full genomic RNA of strain Con1 or strain JFH1 were subjected to immunoblotting using the appropriate antibodies. The asterisk indicates a nonspecific band. (B) Subcellular localizations of LC3 and NS5A were determined by confocal microscopy. The replicon cells and the starved Huh7 cells were stained with DAPI and then reacted with rabbit polyclonal anti-LC3 and mouse monoclonal anti-NS5A antibodies, respectively, followed by Alexa Fluor 488- and 594-conjugated secondary antibodies, respectively. The boxed areas in the merged images are magnified. (C) SGR^{Con1} cells were treated with alpha interferon for 1 week to remove the HCV replicon RNA. The resulting cells were designated SGR^{cured} cells. The SGR^{Con1}, SGR^{cured}, and SGR^{JEV} cells were lysed and subjected to immunoblotting using the appropriate antibodies. (D) Subcellular localization of LC3 and JEV NS3 and HCV NS5A was determined by confocal microscopy after staining with DAPI, followed by staining with rabbit polyclonal anti-LC3 and anti-JEV NS3 antibodies and mouse monoclonal anti-NS5A antibodies and then with the appropriate secondary antibodies. The data shown are representative of three independent experiments.

cells by treatment with the inhibitors, whereas only a slight increase was observed in the SGR^{Con1} cells (5.4-fold versus 1.6-fold) (Fig. 2A), suggesting that autophagy is suppressed in the HCV replicon cells. Furthermore, cytoplasmic accumulation of LC3 was significantly increased in the naïve Huh7 cells by treatment with the inhibitors, in contrast to the only slight increase induced by treatment in the SGR^{Con1} cells (Fig. 2B). In SGR^{Con1} cells, the LC3 foci were colocalized with the polyu-

biquitin-binding protein p62/SQSTM1, a specific substrate for autophagy (18), suggesting that most of the autophagosomes were distributed in the cytoplasm of the SGR^{Con1} cells (Fig. 2B and C). Next, to examine the autophagy flux in the SGR^{Con1} cells, we monitored the green fluorescent protein (GFP)-conjugated LC3 dynamics in living cells by using time-lapse imaging techniques (see movies in the supplemental material). A large number of small GFP-LC3 foci were detected in the
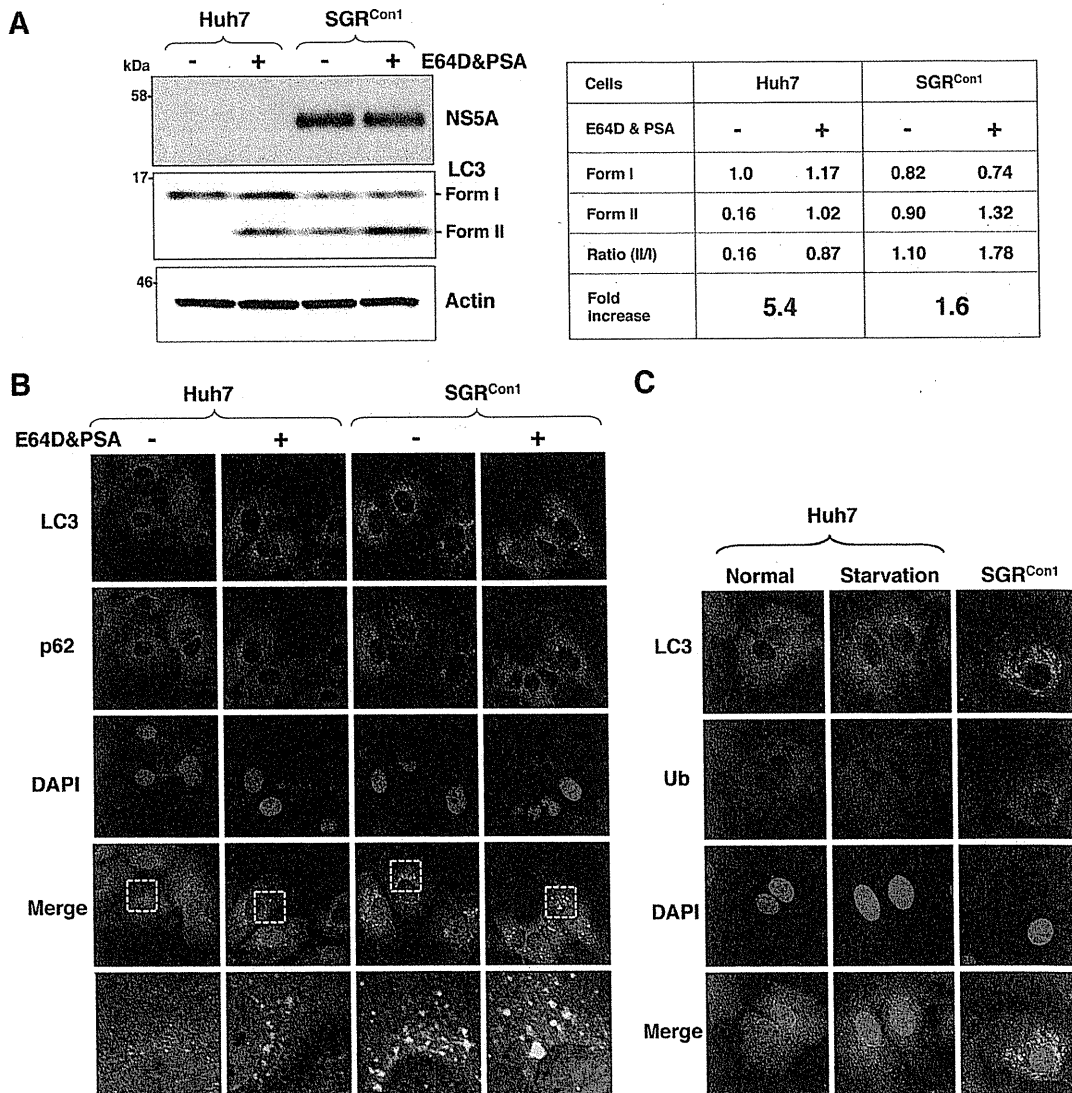
A

Cells	Huh7		SGR^Con1	
E64D & PSA	-	+	-	+
Form I	1.0	1.17	0.82	0.74
Form II	0.16	1.02	0.90	1.32
Ratio (II/I)	0.16	0.87	1.10	1.78
Fold increase	5.4		1.6	

B

C

FIG. 2. Autophagy flux is impaired in the HCV replicon cells. Autophagy flux assay using lysosomal protease inhibitors. (A) Huh7 and SGR^Con1 cells were treated with 20 μM E64D and pepstatin A (PSA) for 6 h, and the cell lysates were subjected to immunoblotting. The density of the protein band was estimated by Multi Gauge version 2.2 (Fujifilm). (B) After nuclear staining with DAPI, the intracellular localizations of LC3 and p62 in each cell were determined by staining with rabbit polyclonal anti-LC3 and mouse monoclonal anti-62 antibodies, respectively, followed by staining with Alexa Fluor 488- and 594-conjugated secondary antibodies, respectively. The resulting cells were observed by confocal microscopy. (C) Colocalization of accumulated LC3 with ubiquitinated proteins (Ub) in SGR^Con1 cells. Nontreated and starved Huh7 cells and SGR^Con1 cells were fixed and stained with DAPI and rabbit anti-LC3 and anti-ubiquitin (6C1.17) (BD) polyclonal antibodies, respectively, and then with the appropriate secondary antibodies. Subcellular localizations of LC3 and Ub were determined by confocal microscopy. The data shown are representative of three independent experiments.

starved Huh7 cell, moved quickly, and finally disappeared within 30 min. Although small foci of GFP-LC3 exhibited characteristics similar to those in the starved cells, some large foci exhibited confined movement and maintained constant fluorescence for at least 3 h in the SGR^Con1 cells. The GFP-LC3 foci in the SGR^JFH1 cells showed characteristics similar to those in the starved cells. These results support the notion that autophagy flux is suppressed in the SGR^Con1 cells at some step after autophagosome formation.

Impairment of autolysosomal acidification causes incomplete autophagy in the replicon cell of strain Con1. Recent

studies have shown that some viruses inhibit the autophagy pathway by blocking the autolysosome formation (10, 42). Therefore, we determined the autolysosome formation in the HCV replicon cells through the fusion of autophagosome with lysosome. Colocalization of small foci of LC3 with LAMP1, a lysosome marker, was observed in the starved Huh7 cells, SGR^Con1 cells, and SGR^JFH1 cells but not in the SGR^cured cells (Fig. 3A), suggesting that autolysosomes are formed in the HCV replicon cells of both Con1 and JFH1 strains. The autolysosome is acidified by the vacuolar-type H^+ ATPase (V-ATPase) and degrades substrates by the lysosomal acidic hy-
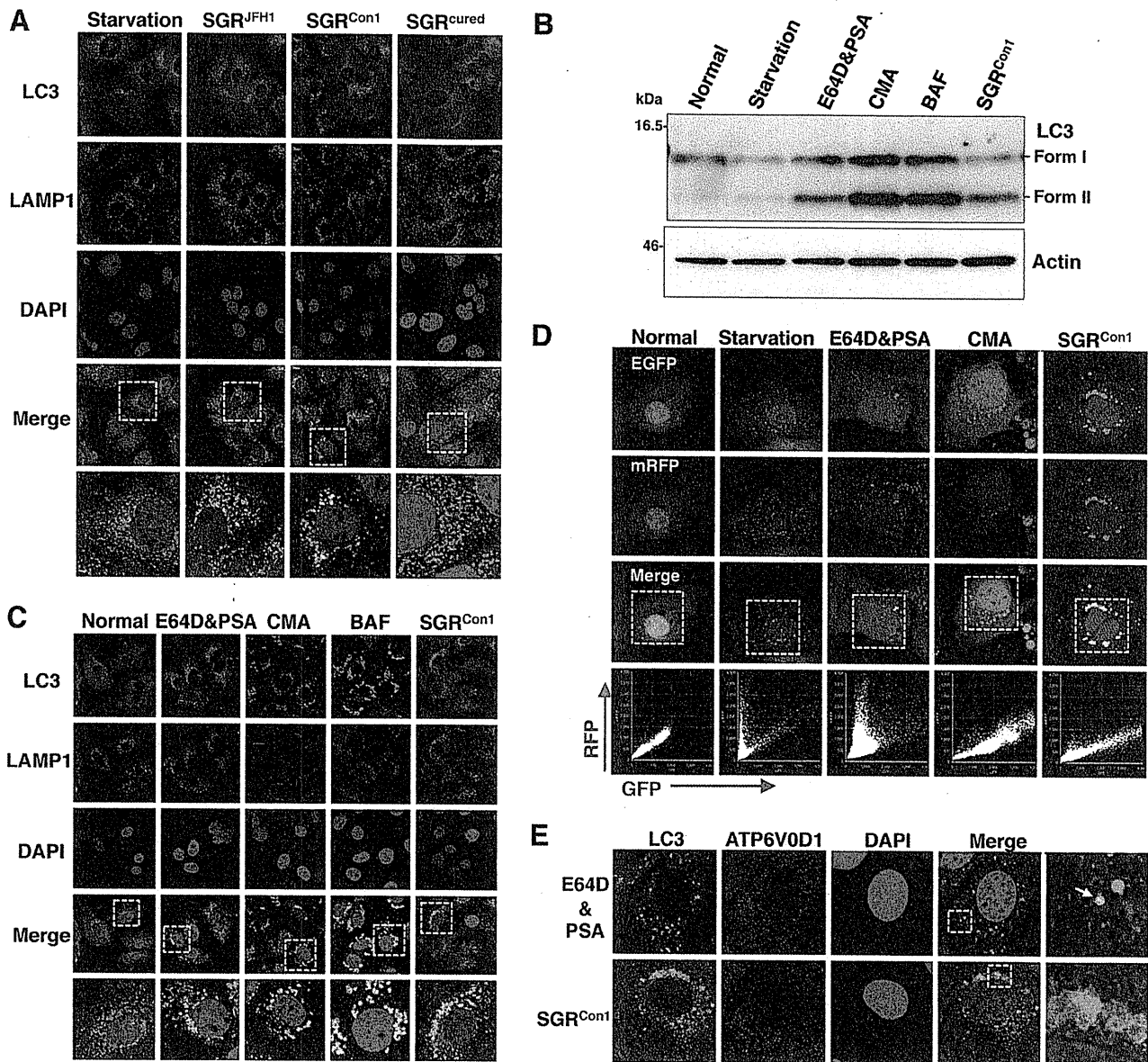
FIG. 3. Inhibition of autophagy maturation in HCV replicon cells. (A) After nuclear staining with DAPI, starved Huh7 cells, replicon cells, and SGR^{cured} cells were stained with rabbit polyclonal anti-LC3 and mouse monoclonal anti-LAMP1 antibodies followed by Alexa Fluor 488- and 594-conjugated secondary antibodies, respectively, and examined by confocal microscopy. The boxed regions in the merged images are magnified. (B and C) Huh7 cells were treated with 20 μM protease inhibitors (E64D and PSA) or a 20 nM concentration of a V-ATPase inhibitor (CMA or BAF) for 6 h. (B) Cell lysates were subjected to immunoblotting using antibodies against LC3 and β-actin. (C) Intracellular localization of LAMP1 and LC3 was determined by confocal microscopy after staining with DAPI and appropriate antibodies. The boxed areas in the merged images are magnified. (D) Tandem fluorescence-tagged LC3 assay. The expression plasmid encoding mRFP-GFP-tandem-tagged LC3 was transfected into naïve and starved Huh7 cells or into the SGR^{Con1} cells treated with the indicated inhibitors at 36 h posttransfection. The resulting cells were fixed at 42 h posttransfection, and the relative GFP and RFP signals were determined by confocal microscopy. The fluorescent values in the boxes of the merged images were determined and shown as dot plots in the bottom column of the grid, in which the x and y axes indicate the signals of GFP and RFP, respectively. (E) Huh7 cells treated with E64D and PSA and the SGR^{Con1} cells were stained with DAPI and then with rabbit polyclonal anti-LC3 and mouse monoclonal anti-ATP6V0D1 antibodies followed by Alexa Fluor 488- and 594-conjugated secondary antibodies, respectively. The boxed regions in the merged images are magnified. A white arrow indicates colocalization of LC3 and ATP6V0D1. The data shown are representative of three independent experiments.

drolases in the vesicle (2). Next, to determine the possibility of a deficiency in the acidification of the autolysosome on the autophagic dysfunction in the Con1 replicon cells, Huh7 cells were treated with the protease inhibitors E64D and pepstatin

A (PSA) or with each of the V-ATPase inhibitors concanamycin A (CMA) and bafilomycin A1 (BAF). The amount of LC3-II was significantly increased in Huh7 cells treated with the inhibitors just as in the SGR^{Con1} cells (Fig. 3B). Further-
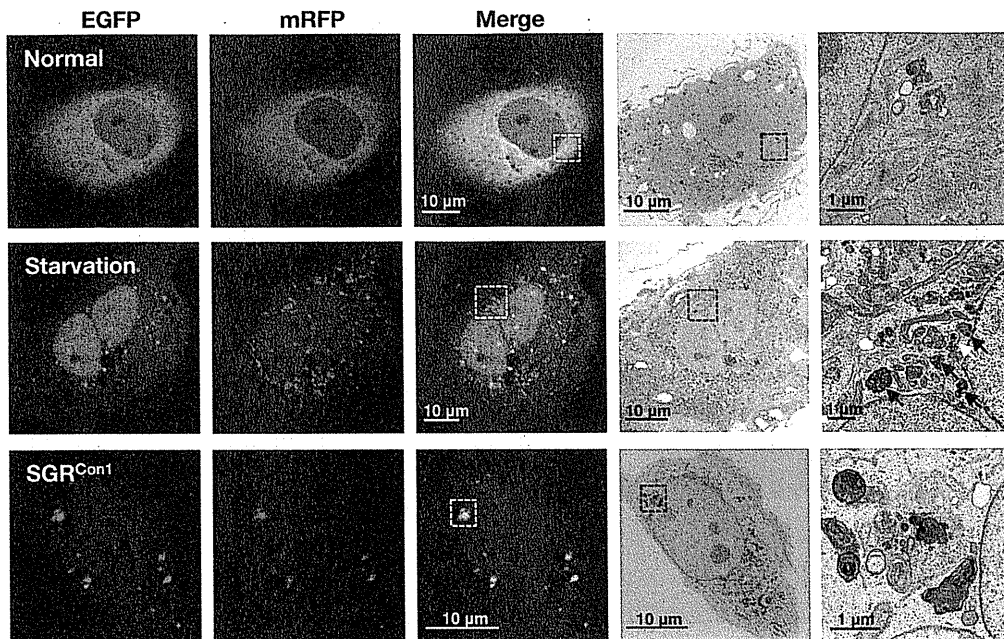
FIG. 4. Correlative fluorescence microscopy-electron microscopy (FM-EM) analysis. The expression plasmid encoding mRFP-GFP-tandem-tagged LC3 was transfected into naïve and starved Huh7 cells or into the SGR^{Con1} cells as described in the legend to Fig. 3D, and the mRFP-GFP-tandem-tagged LC3 signals were observed at 36 h posttransfection. The boxed regions in the merged images are magnified. The data shown are representative of three independent experiments.

more, the large foci of LC3 colocalized with LAMP1 appeared in the cells treated with the V-ATPase inhibitors, as seen in SGR^{Con1} cells (Fig. 3C). These results suggest that stacked autophagosome flux caused by the inhibition of lysosomal degradation or acidification exhibits characteristics similar to those observed in the Con1 replicon cells.

Since the fluorescence of GFP but not that of monomeric red fluorescent protein (mRFP) disappears under the acidic environment, expression of mRFP-GFP tandem fluorescent-tagged LC3 (tfLC3) is capable of being used to monitor the acidic status of the autolysosome (24). Both GFP and mRFP fluorescent signals were unfused, some of them accumulated as small foci in Huh7 cells after starvation or by treatment with the protease inhibitors, and half of the foci of mRFP were not colocalized with those of GFP (Fig. 3D), indicating that half of the foci are in an acidic state due to maturation into an autolysosome after fusion with a lysosome. On the other hand, the large foci of GFP and mRFP were completely colocalized in Huh7 cells treated with CMA or in the SGR^{Con1} cells. These results suggest that the large foci of LC3 in the SGR^{Con1} cells are not under acidic conditions. Recently, it was shown that the lack of lysosomal acidification in human genetic disorders due to dysfunction in assembly/sorting of V-ATPase induces incomplete autophagy similar to that observed in SGR^{Con1} cells (31, 45). Therefore, to explore the reason for the lack of acidification of the autolysosome in the SGR^{Con1} cells, we examined the subcellular localization of ATP6V0D1, a subunit of the integral membrane V$_0$ complex of V-ATPase. Colocalization of ATP6V0D1 with large foci of LC3 was observed in Huh7 cells treated with the protease inhibitors but not in SGR^{Con1} cells (Fig. 3E), suggesting that dislocation of V-

ATPase may participate in the impairment of the autolysosomal acidification in the SGR^{Con1} cells.

We further examined the morphological characteristics of the LC3-positive compartments by using correlative fluorescence microscopy-electron microscopy (FM-EM) (Fig. 4). The starved Huh7 cells exhibited a small double-membrane vesicle (white arrow) and high-density single-membrane structures (black arrows) in close proximity to the correlative position of the GFP- and mRFP-positive LC3 compartments, which are considered to be the autophagosome and lysosome/autolysosome, respectively. In contrast, many high-density membranous structures were detected in the correlative position of the large GFP- and mRFP-positive LC3 compartment in the SGR^{Con1} cells, which is well consistent with the observation in the time-lapse imaging in which small foci of LC3 headed toward and assembled with the large LC3-positive compartment (see movies in the supplemental material). These results suggest that the formation of large aggregates with aberrant inner structures in the SGR^{Con1} cells may impair maturation of the autolysosome through the interference of further fusion with functional lysosomes for the degradation.

The secretion of immature cathepsin B is enhanced in the replicon cell of strain Con1. Lysosomal acidification is required for the cleavage of cathepsins for activation, and cathepsin B (CTSB) is processed under acidic conditions (13). Although a marginal decrease of CTSB was detected in the whole lysates of the SGR^{Con1} cells, a significant reduction in the expression of both unprocessed (pro-CTSB) and matured CTSB was observed in the lysosomal fractions of the SGR^{Con1} cells compared with those of the naïve Huh7 and the SGR^{cured} cells (Fig. 5A). LAMP1 was concentrated at a similar level in
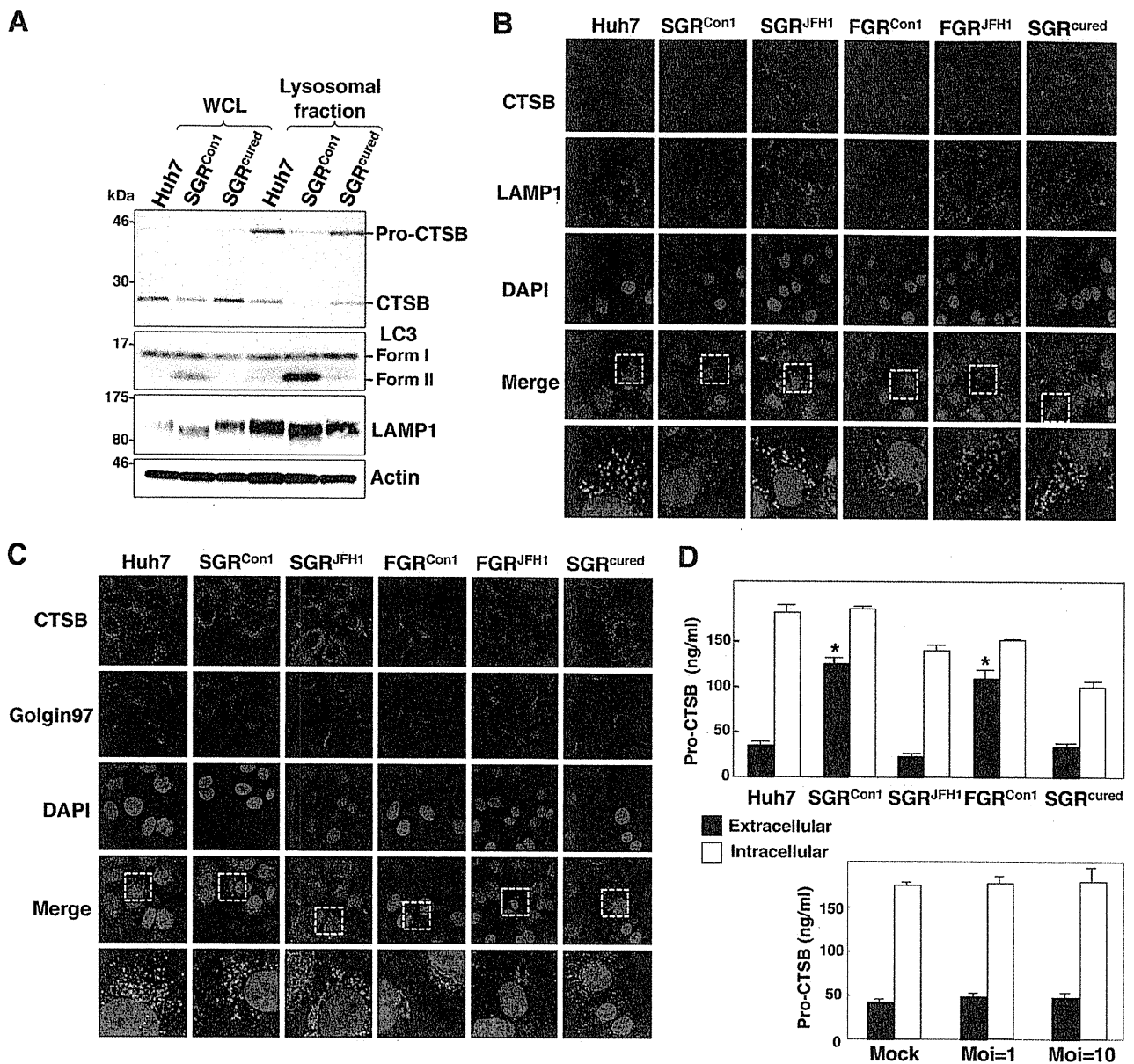
5 5

FIG. 5. Enhanced secretion of pro-CTSB in the HCV replicon cells. (A) The whole-cell lysate (WCL) and lysosomal fraction prepared from Huh7, SGR^{Con1}, and SGR^{cured} cells were subjected to immunoblotting. (B and C) Huh7 cells, HCV replicon cells, and SGR^{cured} cells were stained with DAPI, rabbit polyclonal anti-CTSB antibody, and mouse anti-LAMP1 (B) or anti-Golgin97 (C) antibody. The boxed areas in the merged images are magnified. (D) Expression of pro-cathepsin B in the culture supernatants (black bars) and cell lysates (white bars) of the Huh7, SGR^{Con1}, SGR^{JFH1}, FGR^{Con1}, and SGR^{cured} cells and the SGR^{cured} cells infected with HCVcc at a multiplicity of infection (Moi) of 1 or 10 and incubated for 72 h was determined by enzyme-linked immunosorbent assay (ELISA). The error bars indicate standard deviations. The asterisks indicate significant differences ($P < 0.01$) versus the control value. The data shown are representative of three independent experiments.

the lysosomal fractions of the cells, whereas LC-II was detected in the fractions of the SGR^{Con1} cells but not in those of Huh7 and the SGR^{cured} cells, suggesting that autophagosomes and/or autolysosomes in the SGR^{Con1} cells are fractionated in the lysosomal fraction. Colocalization of CTSB with LAMP1 was observed in the naïve Huh7 cells, in the SGR^{cured} cells, and in the replicon cells harboring a sub- or a full genomic RNA of strain JFH1 (SGR^{JFH1} and FGR^{JFH1}, respectively) but not in those of strain Con1 (SGR^{Con1} and FGR^{Con1}) (Fig. 5B). On

the other hand, CTSB was colocalized with Golgin97, a marker for the Golgi apparatus, in the SGR^{Con1} and FGR^{Con1} cells but not in other cells (Fig. 5C). Since previous reports suggested that the alkalization in the lysosome triggers secretion of the unprocessed lysosomal enzymes (19, 41), we next determined the secretion of pro-CTSB in the replicon cells. Secretion of the pro-CTSB was significantly enhanced in the replicon cells of strain Con1 but not in those of strain JFH1 and naïve and cured cells (Fig. 5D, top). Furthermore, secretion of pro-CTSB

A SGR^Con1 + EV   SGR^Con1 + Atg4B^C74A   SGR^cured + Atg4B^C74A

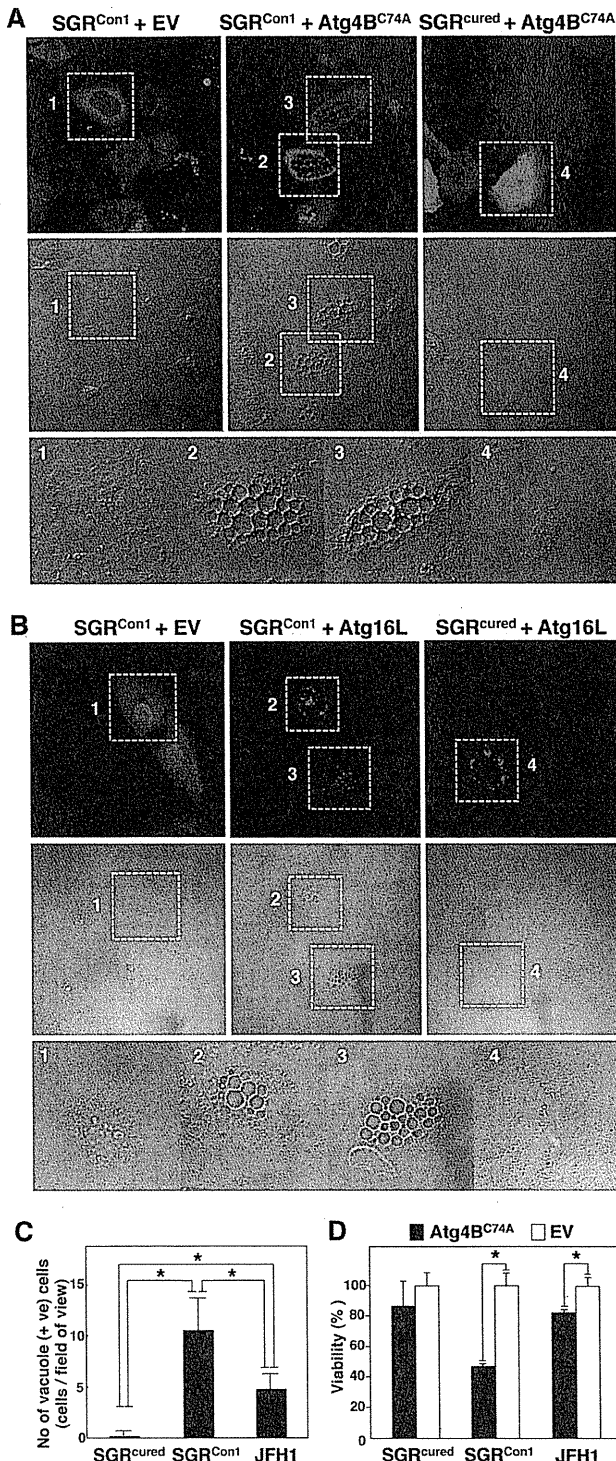**B** SGR^Con1 + EV   SGR^Con1 + Atg16L   SGR^cured + Atg16L

C

D

FIG. 6. Inhibition of autophagosome formation induces severe cytoplasmic vacuolations leading to cell death in the HCV replicon cells. (A) SGR^Con1 and SGR^cured cells transfected with pStrawberry-Atg4B^C74A or empty vector pStrawberry (EV) were fixed at 48 h posttransfection and examined by fluorescence microscopy. The boxed areas in the phase-contrast images are magnified. (B) SGR^Con1 and SGR^cured cells transfected with pEGFP-Atg16L or EV were examined by fluorescence microscopy at 48 h posttransfection. The boxed areas in the phase-contrast images are magnified. (C) SGR^cured, SGR^Con1,

was not observed in the cured cells infected with HCVcc, an infectious HCV strain derived from strain JFH1 (Fig. 5D, bottom). Collectively, these results suggest that the dysfunction of lysosomal acidification contributes to the impairment of autophagy in the HCV replicon cells of strain Con1.

Autophagy induced in cells replicating HCV is required for cell survival. Finally, we examined the pathological significance of autophagy during HCV replication. Atg4B is known as an LC3-processing protease, and overexpression of its protease-inactive mutant (Atg4B^C74A) results in inhibition of the autophagosome formation (7). To our surprise, severe cytoplasmic vacuolation was observed in the SGR^Con1 cells expressing Atg4B^C74A (Fig. 6A). These vacuolations were also observed in the SGR^Con1 cells by the expression of Atg16L (Fig. 6B), a molecule that is an essential component of the autophagy complex and that, if expressed in excess amounts, can disrupt the autophagosome formation (8). Expression of Atg4B^C74A induced a higher level of vacuole formation in the Con1 replicon cells than in cells infected with JFH1 virus but not in the cured cells (Fig. 6C). Along with these vacuolations, cell viability was significantly decreased by the expression of Atg4B^C74A in SGR^Con1 cells and slightly in JFH1 virus-infected cells (Fig. 6D). These results suggest that autophagy induced by the RNA replication of HCV is required for host cell survival.

DISCUSSION

In the present study, we demonstrated that two genotypes of HCV induce autophagy, whereas intact autophagy flux is required for the host cell to survive. The cell death characterized by cytoplasmic vacuolation that was induced in the HCV replicon cells by the inhibition of the autophagosome formation is similar to type III programmed cell death, which is distinguishable from apoptosis and autophagic cell death (4). Type III programmed cell death has been observed in the neurodegenerative diseases caused by the deposit of cytotoxic protein aggregates (15).

We previously reported that HCV hijacks chaperone complexes, which regulates quality control of proteins into the membranous web for circumventing unfolded protein response during efficient genome replication (53); in other words, the replication of HCV exacerbates the generation of proteins associated with cytotoxicity. In the experiments using a chimpanzee model, HCV of genotype 1 was successfully used to reproduce acute and chronic hepatitis similar to that in the human patients (3, 57), and transgenic mice expressing viral proteins of HCV of genotype 1b have been shown to develop

and SGR^cured cells infected with JFH1 virus were transfected with pStrawberry-Atg4B^C74A, and the number of vacuole-positive cells in each of nine fields of view was counted at 48 h posttransfection. (D) SGR^cured, SGR^Con1, and SGR^cured cells infected with JFH1 virus were transfected with pStrawberry-Atg4B^C74A (black bars) or EV (white bars), and cell viability was determined at 6 days posttransfection by using CellTiter-Glo (Promega) according to the manufacturer's protocol. The asterisks indicate significant differences ($P < 0.05$) versus the control value. The data shown are representative of three independent experiments.

Sjögren syndrome, insulin resistance, hepatic steatosis, and hepatocellular carcinoma (27, 28). In contrast, HCVcc, based on the genotype 2a strain JFH1 isolated from a patient with fulminant hepatitis C (33, 56), was unable to establish chronic infection in chimpanzees (56) or to induce cell damage and inflammation in chimeric mice xenotransplanted with human hepatocytes (17). These results imply that the onset of HCV pathogenesis could be dependent not only upon an amount but also on a property of deposited proteins, and they might explain the aggravated vacuolations under the inhibition of autophagosome formation in strain Con1 compared to that in strain JFH1. Interestingly, the overexpression of Atg4B^{C74A} or Atg16L causes eccentric cell death in the Con1 replicon cells in which autophagy flux is already disturbed. Thus, we speculated that the quarantine of undefined abnormalities endowed with high cytotoxicity by the engulfing of the autophagic membrane might be sufficient for the amelioration of HCV-induced degeneration. The autophagosomal dysfunction observed in the Con1 replicon cells may suggest that a replicant of strain Con1 was more sensitive to the lysosomal vacuolation than that of strain JFH1. Because a limitation of our study was that we were unable to use infectious HCV of other strains, it is still unclear whether the autophagic degradation can be impaired only in the replicon of HCV strain Con1 or genotype 1.

We also demonstrated that HCV replication of strain Con1 but not that of strain JFH1 facilitates the secretion of pro-CTSB. It has been well established that the secretion of pro-CTSB is enhanced in several types of tumors (26, 50). The secretion of CTSB, like the secretion of matrix metalloproteases, is a marker of the progression of the proteolytic degradation of the extracellular matrix, which plays an important part in cancer invasion and metastasis. Since infection with HCV of genotype 1 is clinically considered a risk factor for the development of hepatocellular carcinoma (14, 51), the enhanced secretion of pro-CTSB by the replication of genotype 1 strains might synergistically promote infiltration of hepatocellular carcinoma.

As shown elsewhere (see movies in the supplemental material), although most degradations of the autophagosome were impaired due to a dislocalization of a V-ATPase subunit, some autophagic degradation was achieved in the SGR^{Con1} cells similar to that in the starved Huh7 cells. Moreover, the stagnated autophagy flux was rescued by the treatment of alpha interferon accompanied by elimination of HCV (Fig. 1C and D). Interestingly, we observed neither a significant impairment of lysosomal degradation nor the intracellular activity of cathepsins in the replicon cells of HCV strain Con1 (data not shown). Therefore, there might be a specific dysfunction within the autolysosome during the replication of HCV strain Con1. Detailed studies are needed to elucidate how HCV strain Con1 disturbs the sorting of V-ATPase.

A close relationship between autophagy and the immune system has been gradually unveiled (47). Autophagy assists not only in the direct elimination of pathogens by hydrolytic degradation but also in antigen processing in antigen-presenting cells such as macrophage and dendritic cells (DC) for presentation by major histocompatibility complex (MHC) I and II (11). Moreover, autophagy plays important roles in T lymphocyte homeostasis (44). As such, in some instances, interruptions of autophagy can allow microorganisms to escape from

the host immune system. Indeed, the immune response against herpes simplex virus was suppressed by blocking the autophagy (6). With regard to HCV, functionally impaired DC dysfunctions marked by poor DC maturation, impaired antigen presentation, and attenuated cytokine production have been reported in tissue culture models and chronic hepatitis C patients (1, 22, 46). In addition, reduction of cell surface expression of MHC-I in HCV genotype 1b replicon cells has been reported (55). We confirmed that levels of cell surface expression of MHC-I in the replicon cells of genotype 1b, but not of genotype 2a, were reduced in comparison with those in the cured cells (data not shown). Hence it might be feasible to speculate that the replication of HCV RNA of genotype 1 induces an incomplete autophagy for attenuating antigen presentation to establish persistent infection. In contrast, autophagy is known to serve as a negative regulator of innate immunity (21, 54). A recent report demonstrated that autophagy induced by infection with strain JFH1 or dengue virus attenuates innate immunity to promote viral replication (23), indicating that an HCV genotype 2a strain may facilitate autophagy to evade innate immunity.

In this study, we demonstrated that HCV utilizes autophagy to circumvent the cell death induced by vacuole formation for its survival. This unique strategy of HCV propagation may provide new clues to the virus-host interaction and, ultimately, to the pathogenesis of infection by various genotypes of HCV.

REFERENCES

1. **Auffermann-Gretzinger, S., E. B. Keeffe, and S. Levy.** 2001. Impaired dendritic cell maturation in patients with chronic, but not resolved, hepatitis C virus infection. Blood **97:**3171–3176.
2. **Beyenbach, K. W., and H. Wieczorek.** 2006. The V-type H+ ATPase: molecular structure and function, physiological roles and regulation. J. Exp. Biol. **209:**577–589.
3. **Bradley, D. W.** 2000. Studies of non-A, non-B hepatitis and characterization of the hepatitis C virus in chimpanzees. Curr. Top. Microbiol. Immunol. **242:**1–23.
4. **Clarke, P. G.** 1990. Developmental cell death: morphological diversity and multiple mechanisms. Anat. Embryol. (Berl.) **181:**195–213.
5. **Dreux, M., P. Gastaminza, S. F. Wieland, and F. V. Chisari.** 2009. The autophagy machinery is required to initiate hepatitis C virus replication. Proc. Natl. Acad. Sci. U. S. A. **106:**14046–14051.
6. **English, L., et al.** 2009. Autophagy enhances the presentation of endogenous viral antigens on MHC class I molecules during HSV-1 infection. Nat. Immunol. **10:**480–487.
7. **Fujita, N., et al.** 2008. An Atg4B mutant hampers the lipidation of LC3 paralogues and causes defects in autophagosome closure. Mol. Biol. Cell **19:**4651–4659.
8. **Fujita, N., et al.** 2008. The Atg16L complex specifies the site of LC3 lipidation for membrane biogenesis in autophagy. Mol. Biol. Cell **19:**2092–2100.
9. **Fujitani, Y., C. Ebato, T. Uchida, R. Kawamori, and H. Watada.** 2009. β-cell autophagy: a novel mechanism regulating β-cell function and mass: lessons from β-cell-specific Atg7-deficient mice. Islets **1:**151–153.
10. **Gannage, M., et al.** 2009. Matrix protein 2 of influenza A virus blocks autophagosome fusion with lysosomes. Cell Host Microbe **6:**367–380.
11. **Gannage, M., and C. Munz.** 2009. Autophagy in MHC class II presentation of endogenous antigens. Curr. Top. Microbiol. Immunol. **335:**123–140.
12. **Hara, T., et al.** 2006. Suppression of basal autophagy in neural cells causes neurodegenerative disease in mice. Nature **441:**885–889.
13. **Hasilik, A.** 1992. The early and late processing of lysosomal enzymes: proteolysis and compartmentation. Experientia **48:**130–151.